AWARD NUMBER: W81XWH-13-1-0165

TITLE: Pluridirectional High-Energy Agile Scanning Electron Radiotherapy (PHASER): Extremely Rapid Treatment for Early Lung Cancer

PRINCIPAL INVESTIGATOR: Peter. G. Maxim, PhD

CONTRACTING ORGANIZATION: Stanford University
Stanford, CA 94305-2004

REPORT DATE: September 2015

TYPE OF REPORT: Final

PREPARED FOR: U.S. Army Medical Research and Materiel Command
Fort Detrick, Maryland 21702-5012

REPORT DOCUMENTATION PAGE

Form Approved
OMB No. 0704-0188

1. REPORT DATE	2. REPORT TYPE	3. DATES COVERED
September 2015	Final	15 Jun 2013- 14 Jun 2015

4. TITLE AND SUBTITLE
Pluridirectional High-Energy Agile Scanning Electron Radiotherapy (PHASER): Extremely Rapid Treatment for Early Lung Cancer

5a. CONTRACT NUMBER
W81XWH-13-1-0165

5b. GRANT NUMBER

5c. PROGRAM ELEMENT NUMBER

6. AUTHOR(S)
Peter G Maxim, PhD
Billy W Loo, MD, PhD

E-Mail: pmaxim@stanford.edu, bwloo@stanford.edu

5d. PROJECT NUMBER

5e. TASK NUMBER

5f. WORK UNIT NUMBER

7. PERFORMING ORGANIZATION NAME(S) AND ADDRESS(ES)
Stanford University
450 Serra Mall
Stanford, CA 94305-2004

8. PERFORMING ORGANIZATION REPORT NUMBER

9. SPONSORING / MONITORING AGENCY NAME(S) AND ADDRESS(ES)
U.S. Army Medical Research and Materiel Command
Fort Detrick, Maryland 21702-5012

10. SPONSOR/MONITOR'S ACRONYM(S)

11. SPONSOR/MONITOR'S REPORT NUMBER(S)

12. DISTRIBUTION / AVAILABILITY STATEMENT
Approved for Public Release; Distribution Unlimited

13. SUPPLEMENTARY NOTES

14. ABSTRACT

We propose to develop a new type of radiotherapy (RT) system for early stage lung cancer using rapidly scanned beams from many directions through electromagnetic steering with no mechanical moving parts, referred to as **pluridirectional high-energy agile scanning electron radiotherapy (PHASER)**. Such a system would be similar in size and cost to commonly available systems, but would deliver an entire treatment of high-dose RT in less than one second, and with even sharper dose sculpting than the current state-of-the-art. In addition, extremely rapid radiation delivery may have a more effective biological impact on tumors for the same radiation dose. We have established a unique multidisciplinary collaboration between Stanford University Department of Radiation Oncology and the Accelerator Research Division at Stanford Linear Accelerator Center (SLAC) National Accelerator Laboratory, to design such a system.

15. SUBJECT TERMS
lung cancer, radiotherapy, biological effectiveness, high energy electrons

16. SECURITY CLASSIFICATION OF:			17. LIMITATION OF ABSTRACT	18. NUMBER OF PAGES	19a. NAME OF RESPONSIBLE PERSON
a. REPORT	b. ABSTRACT	c. THIS PAGE			USAMRMC
U	U	U	UU	64	19b. TELEPHONE NUMBER *(include area code)*

Table of Contents

Page

Contract number: W81XWH-13-1-0165

Title: High-Energy Agile Scanning Electron Radiotherapy (PHASER): Extremely Rapid Treatment for Early Lung Cancer

Principal Investigator: Peter G Maxim, PhD

Introduction:

Cancer is the leading cause of death worldwide and is **increasing epidemically** because of multiple factors including population aging and growth. **Radiation therapy (RT) is a primary curative treatment modality** for cancer whose therapeutic **role and effectiveness are increasing** because of major advances intechnology, molecularly targeted drug therapy, and immunotherapy among others. In addition, novel applications of ad- vanced RT for major non-cancer illnesses are rapidly emerging. However, access to RT falls far short ofthe need for it worldwide and **this gap is growing rapidly**.

We are developing the next generation RT concept, **pluridirectional high-energy agile scanning electron radiotherapy (PHASER)**. The key breakthroughs of the PHASER paradigm are extreme treatment speed that both enables unprecedented accuracy by eliminating the problem of physiologic motion and increases patient throughput; compact and economical design that makes it broadly practical and accessible; improved dose dis- tribution compared to best existing photon therapy based on the use of very high-energy electron (VHEE) beams; and potentially enhanced biological effectiveness. **We envision PHASER as a viable replacement for nearly all existing RT systems, improving clinical effectiveness, cost effectiveness, and availability of curative RT for millions of patients with cancer and other major illnesses in the U.S. and globally.**

We have assembled a research team comprising investigators from the Stanford Department of Radiation On- cology with world-class expertise in clinical radiation oncology, medical physics, and cancer and radiation biol- ogy and who have initiated world's first clinical trials of stereotactic ablative radiotherapy for cancer and major pulmonary and cardiovascular diseases, from the Department of Radiology with world-class expertise in imag- ing system design, and from the SLAC National Accelerator Laboratory with world-class expertise in compact high-energy linear accelerator design, leveraging **talent and resources that can be found nowhere else in the world**.
Our specific aims in this proposal are to produce a practically realizable PHASER design through simulation and experimental validation.

Body:

<u>Task 1 - Specific Aim 1:</u> To determine optimal operating parameters for PHASER using Monte Carlo simu-
lations (months 1-22)

Task 1a: We will perform simulations using an array of MC codes well established in particle physicsre- search: GEANT4, Monte Carlo N-Particle eXtended (MCNPX) and the extension of the Electron Gamma Shower code developed at the National Research Council Canada (EGSnrc). This will permit cross validation of codes and also simulation of electronuclear and photonuclear interac- tions not available in all of the codes (months 1-5).

Task 1b: Clinical scenarios: We will simulate treatment of 4 different body regions with varying tissue characteristics – head/neck, thorax (lung), abdomen (liver), and pelvis (prostate) – using repre- sentative CT data sets for each site. In each site, we will simulate both focal and extended (lo- cally advanced) tumor targets (months 5-12).

Task 1c: Treatment planning and plan evaluation: PHASER plans will be manually optimized by forward planning. They will be compared with the best achievable photon VMAT plans in each case.
Comparisons will be made by normalizing all plans to achieve the same volumetric coverage (95%) of the planning target volume (PTV) by the prescription dose, and comparing the con- formity index at various isodose levels, defined as the ratio of the respective isodose volume to the PTV. In addition, we will code a treatment plan optimizer in MATLAB based on published lit- erature (month 13-17).

Task 1d: Treatment planning optimization: We will develop an in-house inverse treatment planning optimiza- tion system based on simulated annealing and Monte Carlo simulations. We will use the optimiza- tion schemes for comparison of optimized PHASER treatment plans to state-of-the-art photon VMAT plans. We will also investigate the impact of variables such as body habits and implanted prostheses.

Status Specific Aim 1:

We have developed a software interface to allow high-accuracy Monte Carlo simulations of VHEE dose calculations to be set up and imported into an advanced commercial treatment planning system (provided by RaySearch Labor- atories, through an established research collaboration) which allows complete inverse planning optimization. This allows us to produce treatment plans as though PHASER were clinically available, and compare these treatment plans with the best current photon-based plans. We have now simulated treatments of a broad range of anatomic sites, including head and neck, lung, liver, pelvis (with and without metallic prosthetic implants), and pediatric brain, including both small and extended field targets. We have completed Task 1 and we have an accepted manuscript in Medical Physics (*Treatment planning for radiotherapy with very high-energy electron beams and comparison of VHEE and VMAT plans*, Bazalova et al) and one manuscript currently under review in Radiotherapy and Oncolo- gy (*Assessment of the quality of very high-energy electron radiotherapy treatment planning: Five clinical cases,* Palma et al*),* detailing our results of Task 1. The manuscripts, acknowledging DoD support, are attached to this re- port.

This work was **selected for three oral presentations (one as a Featured Presentation) and a poster at the 2014 and 2015 American Association for Physicists in Medicine (AAPM) annual meeting.**

Task 2 - Specific Aim 2: To perform experimental validation and calibration of the Monte Carlo codes at NLCTA (SLAC) (months 10-22)

Task 2a: Homogeneous phantom measurements: As described in our preliminary results above, we have constructed a homogeneous phantom using slabs of tissue equivalent polystyrene plastic, be- tween which films can be inserted to record the dose profiles. We will measure beam profiles for field sizes ranging from 0.1-5 cm and electron energies ranging from 50-100 MeV (months 8- 15).

Task 2b Heterogeneous phantom measurements: We will construct a series of heterogeneous phantoms consisting of slabs of polystyrene stacking to form a 15 cm cube, with features of various densi- ties inserted to simulate different tissue types (months 15-22).

Status Specific Aim 2:

We have completed Task2a and have an accepted manuscript in Medical Physics detailing our results of homoge- nous phantom measurements (*Comparison of film measurements and Monte Carlo simulations of dose deliv- ered with very high-energy electron beams in a polystyrene phantom*, Bazalova et al.). The submitted manu- script, acknowledging DoD support, is attached to this report.

Task 3: Data analysis and submission for publication in peer reviewed journal (months 23-24).

Three manuscripts summarizing the results of the tasks outlined in this proposal are published in peer re- viewed journals and attached to this report.

Key Research Accomplishments:

- We have developed a software interface for Monte Carlo calculations.
- We have established a research collaboration with RaySearch Laboratories that includes a license for their commercially available treatment planning system, which allows inverse planning optimization.
- We have demonstrated proof of principle that 80-100 MeV electrons consistently produce equal or superior dose distributions compared with the best clinically used photo VMAT plans.
- We have completed the tasks and published three manuscripts, detailing the results of this proposal.

Reportable Outcomes:

The following abstracts have been selected for oral/poster presentation at the 56th and 57th Annual Meeting of the American Association of Physicists in Medicine (AAPM):

1) FEATURED PRESENTATION - Treatment Planning Tool for Radiotherapy with Very High-Energy Electron Beams

M Bazalova[1]*, B Qu[1], E Hynning[2], B Hardemark[2], B Palma[1], B Loo[1], P Maxim[1], (1) Stanford University, Stanford, CA, (2) RaySearch Laboratories, Stockholm, Sweden

Purpose: To develop a tool for treatment planning optimization for fast radiotherapy delivered with very high- energy electron beams (VHEE) and to compare VHEE plans to state-of-the-art plans for challenging pelvis and H&N cases.

Methods: Treatment planning for radiotherapy delivered with VHEE scanning pencil beams was performed by integrating EGSnrc Monte Carlo (MC) dose calculations with spot scanning optimization run in a research ver- sion of RayStation. A Matlab GUI for MC beamlet generation was developed, in which treatment parameters such as the pencil beam size and spacing, energy and number of beams can be selected. Treatment planning study for H&N and pelvis cases was performed and the effect of treatment parameters on the delivered dose distributions was evaluated and compared to the clinical treatment plans. The pelvis case with a 691cm3 PTV was treated with 2-arc 15MV VMAT and the H&N case with four PTVs with total volume of 531cm3 was treated with 4-arc 6MV VMAT.

Results: Most studied VHEE plans outperformed VMAT plans. The best pelvis 80MeV VHEE plan with 25 beams resulted in 12% body dose sparing and 8% sparing to the bowel and right femur compared to the VMAT plan. The 100MeV plan was superior to the 150MeV plan. Mixing 100 and 150MeV improved dose sparing to the bladder by 7% compared to either plan. Plans with 16 and 36 beams did not significantly affect the dose distributions compared to 25 beam plans. The best H&N 100MeV VHEE plan decreased mean doses to the brainstem, chiasm, and both globes by 10-42% compared to the VMAT plan.

Conclusion: The pelvis and H&N cases suggested that sixteen 100MeV beams might be sufficientspecifica- tions of a novel VHEE treatment machine. However, optimum machine parameters will be determined with the presented VHEE treatment-planning tool for a large number of clinicalcases.

2) The Effect of Beam Parameters On Very High-Energy Electron Radiotherapy: A Planning Study

B Palma[1]*, M Bazalova[1], B Hardemark[2], E Hynning[2], B Qu[1], B Loo[1], P Maxim[1], (1)Department of Ra- diation Oncology, Stanford University, Stanford, CA, (2) RaySearch Laboratories AB, Stockholm, Swe- den

Purpose: We evaluated the effect of very high-energy electron (VHEE) beam parameters on the planning of a lung cancer case by means of Monte Carlo simulations.

Methods: We simulated VHEE radiotherapy plans using the EGSnrc/BEAMnrc-DOSXYZnrc code. We selected a lung cancer case that was treated with 6MV photon VMAT to be planned with VHEE. We studied the effect of beam energy (80 MeV, 100 MeV, and 120 MeV), number of equidistant beams (16 or 32), and beamlets sizes (3 mm, 5 mm or 7 mm) on PTV coverage, sparing of organs at risk (OARs) and dose conformity. Inverse- planning optimization was performed in a research version of RayStation (RaySearch Laboratories AB) using identical objective functions and constraints for all VHEE plans.

Results: Similar PTV coverage and dose conformity was achieved by all the VHEE plans. The 100 MeV and 120 MeV VHEE plans were equivalent amongst them and were superior to the 80 MeV plan in terms of OARs sparing. The effect of using 16 or 32 equidistant beams was a mean difference in average dose of 2.4% (0%- 7.7%) between the two plans. The use of 3 mm beamlet size systematically reduced the dose to all the OARs. Based on these results we selected the 100MeV-16beams-3mm-beamlet-size plan to compare it against VMAT. The selected VHEE plan was more conformal than VMAT and improved OAR sparing (heart and tra- chea received 125% and 177% lower dose, respectively) especially in the low-dose region.

Conclusion: We determined the VHEE beam parameters that maximized the OAR dose sparing and dose con- formity of the actually delivered VMAT plan of a lung cancer case. The selected parameters could be used for the planning of other treatment sites with similar size, shape, and location. For larger targets, a larger beamlet size might be used without significantly increasing the dose.

3) Radiation Therapy with Very High-Energy Electron (VHEE) Beams in the Presence of Metal Implants
(Poster presentation)

C Jensen[1]*, B Palma[1], B Qu[1], P Maxim[1], B Hardemark [2], E Hynning [2], B Loo[1], M Bazalova[1], (1)Department of Radiation Oncology, Stanford University, Stanford, CA, (2) RaySearch Laboratories, Stockholm, Sweden

Purpose: To evaluate the effect of metal implants on treatment plans for radiation therapy with very high- energy electron (VHEE) beams.

Methods: The DOSXYZnrc/BEAMnrc Monte Carlo (MC) codes were used to simulate 50-150MeV VHEE beam dose deposition and its effects on steel and titanium (Ti) heterogeneities in a water phantom. Heterogeneities of thicknesses ranging from 0.5cm to 2cm were placed at 10cm depth. MC was also used to calculate electron and photon spectra generated by the VHEE beams' interaction with metal heterogeneities. The original VMAT patient dose calculation was planned in Eclipse. Patient dose calculations with MC-generated beamlets were planned using a Matlab GUI and research version of RayStation. VHEE MC treatment planning was performed on water-only geometry and water with segmented prostheses (steel and Ti) geometries with 100MeV and 150MeV beams.

Results: 100MeV PDD 5cm behind steel/Ti heterogeneity was 51% less than in the water-only phantom. For some cases, dose enhancement lateral to the borders of the phantom increased the dose by up to 22% in steel and 18% in Ti heterogeneities. The dose immediately behind steel heterogeneity decreased by an average of 6%, although for 150MeV, the steel heterogeneity created a 23% increase in dose directly behind it. The average dose immediately behind Ti heterogeneities increased 10%. The prostate VHEE plans resulted in mean dose decrease to the bowel (20%), bladder (7%), and the urethra (5%) compared to the 15MV VMAT plan. The average dose to the body with prosthetic implants was 5% higher than to the body without implants.

Conclusion: Based on MC simulations, metallic implants introduce dose perturbations to VHEE beams from lateral scatter and backscatter. However, when performing clinical planning on a prostate case, the use of mul- tiple beams and inverse planning still produces VHEE plans that are dosimetrically superior to photon VMAT plans.

Conclusion:

We have made significant progress towards the proposed project. We have demonstrated that the computa- tional tools (Monte Carlo codes) are adequate to simulate the interaction of VHEE in tissue and phantoms. We have also demonstrated proof of principle that for diverse clinical scenarios, VHEE in the practically achievable energy range of 80-100 MeV consistently produces equal or superior dose distributions compared with the best clinically used photon VMAT plans.

3) Evaluation of the performance of very high-energy electron (VHEE) beams in radiotherapy: Five clin- ical cases

Bianey Palma[1], Magdalena Bazalova-Carter[1], Bjorn Hårdemark[2], Elin Hynning[2], Bradley Qu[1], Peter G. Maxim[1], and Billy W. Loo, Jr.[1]

(1) Department of Radiation Oncology, Stanford University, Stanford, CA 94305, USA
(2) RaySearch Laboratories AB, Stockholm, Sweden

Purpose/Objective(s): To evaluate the performance of 100-120 MeV very-high energy electron (VHEE) scan- ning pencil beams to radiotherapy by means of Monte Carlo (MC) simulations.

Materials/Methods: We selected five clinical cases with target sizes of 1.2 cm^3 to 990.4 cm^3. We calculated VHEE treatment plans using the MC EGSnrc code implemented in a MATLAB-based graphical user interface developed by our group. We generated phase space data for beam energies: 100 and 120 MeV, pencil beam spot sizes of 1, 3, and 5 mm at FWHM, and number of equidistant beams of 16 or 32. Dose was calculated and then imported into a research version of RayStation where inverse-planning optimization was performed. We compared the VHEE plans with the clinically delivered volumetric modulated arc therapy (VMAT) plan to evaluate VHEE plans performance.

Results: VHEE plans provided the same PTV coverage and dose homogeneity than VMAT plans for all the cases. In average, the mean dose to organs at risk (OARs) was 23.8% lower for the VHEE plans. The struc- tures that benefited the most from using VHEE were: large bowel for the esophagus case, chest wall for the liver case, brainstem for the acoustic case, carina for the lung case, and genitalia for the anal case, with 34.6%, 29.1%, 26.7%, 25.8%, and 23.7% lower dose, respectively. VHEE dose distributions were more con- formal than VMAT solution as confirmed by conformity indices CI_{100} and CI_{50}. Integral dose to the body was in average 19.6% (9.2%-36.5%) lower for the VHEE plans.

Conclusions: We have shown that VHEE plans resulted in similar or superior dose distributions compared to clinical VMAT plans for five different cases including a case with a small target (1.2 cm^3), which represents a challenge even for VMAT planning and might require the use of a more sophisticated photons radiotherapy technique.

Appendix:

Comparison of film measurements and Monte Carlo simulations of dose delivered with very high-energy electron beams in a polystyrene phantom

Magdalena Bazalova-Carter, Michael Liu, and Bianey Palma
Department of Radiation Oncology, Stanford University, Stanford, California 94305-5847

Michael Dunning, Doug McCormick, Erik Hemsing, Janice Nelson, Keith Jobe, and Eric Colby[a)]
SLAC National Accelerator Laboratory, Menlo Park, California 94025

Albert C. Koong
Department of Radiation Oncology, Stanford University, Stanford, California 94305-5847

Sami Tantawi and Valery Dolgashev
SLAC National Accelerator Laboratory, Menlo Park, California 94025

Peter G. Maxim[b)] and Billy W. Loo, Jr.[b)]
Department of Radiation Oncology, Stanford University, Stanford, California 94305-5847

(Received 19 June 2014; revised 17 December 2014; accepted for publication 8 February 2015; published 17 March 2015)

Purpose: To measure radiation dose in a water-equivalent medium from very high-energy electron (VHEE) beams and make comparisons to Monte Carlo (MC) simulation results.
Methods: Dose in a polystyrene phantom delivered by an experimental VHEE beam line was measured with Gafchromic films for three 50 MeV and two 70 MeV Gaussian beams of 4.0–6.9 mm FWHM and compared to corresponding MC-simulated dose distributions. MC dose in the polystyrene phantom was calculated with the EGSnrc/BEAMnrc and DOSXYZnrc codes based on the experimental setup. Additionally, the effect of 2% beam energy measurement uncertainty and possible non-zero beam angular spread on MC dose distributions was evaluated.
Results: MC simulated percentage depth dose (PDD) curves agreed with measurements within 4% for all beam sizes at both 50 and 70 MeV VHEE beams. Central axis PDD at 8 cm depth ranged from 14% to 19% for the 5.4–6.9 mm 50 MeV beams and it ranged from 14% to 18% for the 4.0–4.5 mm 70 MeV beams. MC simulated relative beam profiles of regularly shaped Gaussian beams evaluated at depths of 0.64 to 7.46 cm agreed with measurements to within 5%. A 2% beam energy uncertainty and 0.286° beam angular spread corresponded to a maximum 3.0% and 3.8% difference in depth dose curves of the 50 and 70 MeV electron beams, respectively. Absolute dose differences between MC simulations and film measurements of regularly shaped Gaussian beams were between 10% and 42%.
Conclusions: The authors demonstrate that relative dose distributions for VHEE beams of 50–70 MeV can be measured with Gafchromic films and modeled with Monte Carlo simulations to an accuracy of 5%. The reported absolute dose differences likely caused by imperfect beam steering and subsequent charge loss revealed the importance of accurate VHEE beam control and diagnostics.
 [http://dx.doi.org/10.1118/1.4914371]

Key words: Monte Carlo, dose calculations, very high-energy electrons

1. INTRODUCTION

External beam radiation therapy has been historically most frequently delivered with medical linear accelerators generating photon and electron beams with energies in the range between 5 and 20 MeV. Megavoltage (MV) photon beams of these energies have suitable attenuation and dose deposition properties for treatments of deep-seated tumors.[1] Electron beams of similar energy, however, deposit a large fraction of their energy on the skin and are mostly used for treatments of superficial cancers.[2,3]

Previous work has demonstrated, in principle, a number of advantages of using very high-energy (50–250 MeV) electron (VHEE) beams for radiation therapy of deep-seated tumors.[4–7] Monte Carlo (MC) simulations with the [redacted] (Refs. 8 and 9) code showed that electron beams of such high energies have similar to superior dose deposition properties compared to currently clinically used photon beams. For example, intensity-modulated VHEE therapy for prostate cancer at 250 MeV energy outperformed intensity-modulated radiation therapy (IMRT) with 15 MV photon beams.[7]

The dosimetric advantages of VHEE stem from favorable depth-dose characteristics relative to photons, with a flatter initial profile to clinically relevant depths, followed by a more rapid falloff with a range that depends on the beam energy. Additionally, the reduced dose perturbations at interfaces between media of different density result in much less sensitivity to tissue heterogeneity.[4] Thus, when multiple

beams are used, higher conformity and lower integral dose for the same target coverage is possible with VHEE compared to photons, intermediate between photons and protons, and with less concern about underdosing in buildup regions or range uncertainty issues.

MC simulation is the core methodology for dose calculation of VHEE for potential radiation therapy applications. To date, however, there has been minimal comparison of Monte Carlo codes to experimental data for electrons in the 50–100 MeV energy range in tissue equivalent materials, due mainly to lack of availability of VHEE beams experimentally.[4] Experimental dose measurements and MC dose calculations with the DPM code up to 50 MeV from the racetrack microtron have been published.[10–12] In this work, we present experimental measurements of dose deposition of 50 and 70 MeV VHEE beams in a homogeneous phantom acquired at an experimental beam line and compared them to EGSnrc[13] MC simulations. We also performed absolute dose comparison for MC simulations and experimental measurements of VHEE beams, a challenging task not previously attempted in prior work on VHEE dosimetry, in order to understand the limits of our current experimental system more completely.

2. MATERIALS AND METHODS

2.A. Experimental measurements on a VHEE beam line

Measurements of VHEE beam percentage depth-dose curves (PDDs) and dose profiles were performed at the Next Linear Collider Test Accelerator (NLCTA) located at the SLAC National Accelerator Laboratory.[14] The electron beam is produced by an S-band RF photoinjector, is further accelerated by two high-gradient *X* -band RF accelerating structures, and is transported approximately 25 m to the experimental station inside a beam line with aperture varying from 6 to 20 mm. There are several quadrupole and dipole magnets to assist in beam transport, and diagnostics to monitor beam energy, energy spread, charge, beam size, and beam position.

The NCLTA beam line was modified to accommodate the experimental setup. A 50-μm thick vacuum window of 1.27 cm in diameter made of stainless steel was used to interface the beam line with open air, in which a dose phantom was placed. Dose distributions of 50 and 70 MeV beams were measured using radiochromic films that were embedded in the polystyrene phantom [Figs. 1(a) and 1(b)]. The beam energy was monitored using a large electro-magnet and a phosphorescent screen. Two thin scintillator screens placed in the front and behind the phantom were used to monitor the beam size that was controlled with magnets located upstream from the exit window. The scintillator screens were moved out of the beam line when the phantom was irradiated. The various beam sizes [expressed as full width at half maximum (FWHM) throughout the manuscript] and shapes measured by the film at 0.64 cm depth are shown in Fig. 1(c).

The dose phantom consisted of stacked polystyrene $(C_8H_8)_n$ slabs with mass density of 1.05 g/cm^3, which is comparable to water. Sheets of Gafchromic EBT2 dosimetry film (ISP, Wayne, NJ) were placed at nine depths ranging from 0.64 to 8.7 cm with 0.64, 1.27, and 1.91 cm spacing, as demonstrated in Fig. 1(a). The phantom was placed 15 cm away from the beam line exit window.

Magnets upstream of the steel exit window were used to alter the beams' FWHM, allowing for three beam sizes at each of the two energies. Nominally, the beam FWHMs were chosen to be 5, 3, and 2 mm for the 50 MeV beam and 2 and 1 mm for the 70 MeV beam. However, accurate adjustment of the beam FWHM was not possible with the existing beam diagnostics equipment, and actual beam FWHMs (including the effects of scattering by the exit window and air) were determined on the film at depth of 0.64 cm in the phantom. The number of pulses was altered based on MC simulations to approximately achieve similar film doses using 40, 20, and 10 pulses at 50 MeV and 40 and 20 pulses at 70 MeV. The charge of each pulse was nominally 30 pC, or $\sim 1.87 \times 10^8$ electrons/pulse. Each pulse was 1 ps long and pulses were delivered with 1 Hz repetition rate.

The irradiated Gafchromic EBT2 films were digitized on a Perfection V500 flatbed scanner (EPSON, Long Beach, CA) with 254-dpi resolution. The film was calibrated using a 12 MeV electron beam generated by a clinical linear accelerator (Trilogy, Varian Medical System, Palo Alto, CA).

2.B. Monte Carlo modeling of VHEE experiment

The EGSnrc BEAMnrc/DOSXYZnrc MC codes were selected to model the experimental setup.[15,16] The steel window and the polystyrene phantom were included in the simulations. At first, normally incident monodirectional beams of 2D Gaussian spatial spread were assumed. Electron pencil beams passing through the steel window were simulated in the BEAMnrc code and dose deposition in phantoms was simulated with the BEAMnrc-generated phase-space file in the DOSXYZnrc code. According to the experimental setup, the window to phantom distance was set to 15 cm. A voxel size of $0.5 \times 0.5 \times 0.5$ mm^3 was used for dose scoring and the number of primary electrons used for each simulation was set to 1×10^7. All interactions, including triplet production, photonuclear attenuation, radiative Compton correction, electron impact ionization, and Rayleigh scattering were included in the simulations. Electrons and photons were transported down to kinetic energy of 10 keV. The measured and calculated dose distributions were compared by means of PDD curves and beam profiles at four depths using | | | | | | (The Mathworks, Natick, MA).

2.C. Monte Carlo modeling of beam angular spread

The presence of the steel window in the beam line significantly increased the angular spread of the low-emittance input electron beam. Since the dimensions of the accelerated electron beam could not be measured accurately, the angular spread was investigated by simulating a range of phantom

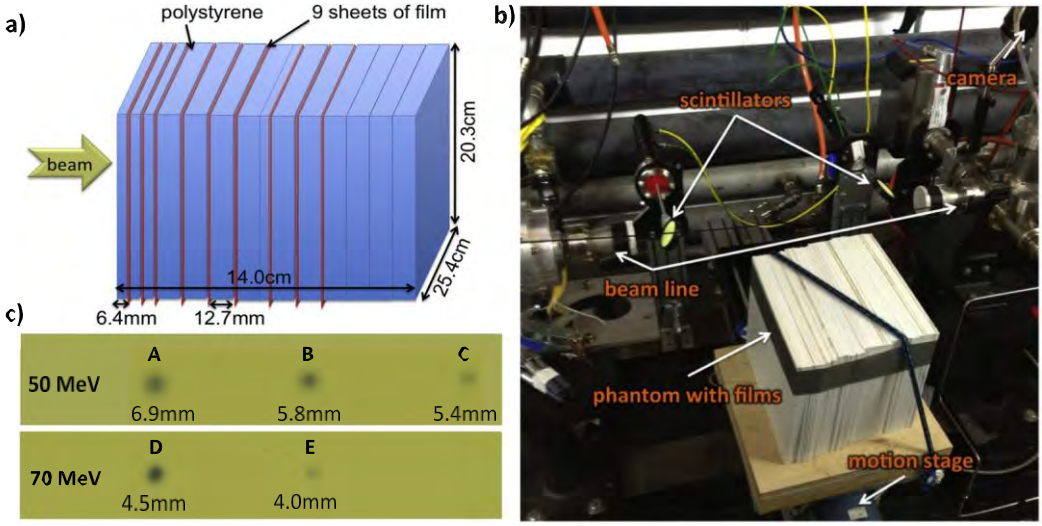

F . 1. Schematics (a) and a photograph (b) of the experimental setup for measurements of 50 and 70 MeV VHEE beams with Gafchromic EBT2 films (c) at the NLCTA beam line of SLAC National Accelerator Laboratory. Films were sandwiched in a 14-cm deep polystyrene phantom and irradiated at five locations with pencil beams of FWHMs ranging from 4.0 to 6.9 mm as measured on the film at 0.64 cm depth (c).

incident Gaussian beam widths and calculating the expected beam profile at the location of the film at 0.64 cm depth in the phantom positioned 15 cm from the exit window. From this relationship, the experimental input beam widths were back-calculated from the film measurements based on a second order polynomial fit applied to the data.

The effects of angular beam spread and VHEE beam energy distribution on the measured dose distribution were also investigated by means of MC simulations. Specifically, central-axis depth dose of the largest beam sizes for both beam energies were simulated with the maximum possible energy spread and angular beam spread. The maximum possible angular beam spread of 0.286° was estimated from the 60 cm distance between the first upstream electromagnet to the exit window and the 6 mm FWHM beam that passes through the exit window without being clipped. Due to the energy measurement accuracy of 2%, dose distributions for 50.0 ± 1.0 MeV and 70.0 ± 1.4 MeV were simulated. Similarly, the effect of the 0.25% FWHM energy spread on dose distributions of the largest beams was studied.

2.D. Monte Carlo modeling of x-ray contamination due to the exit window

The amount of x-ray production in the steel exit window was determined, in order to evaluate the effect of exit window x-ray contamination on dose depositions of the studied 50 and 70 MeV electron beams. Electron beams with 50 and 70 MeV of 2-mm FWHM interacted with the 50-μm thick steel window and phase-space files downstream of the steel window were scored. Central-axis PDD in a water phantom calculated only with x-rays generated in the exit window was compared to the central-axis PDD calculated with all particles in the phase-space file.

2.E. Monte Carlo modeling of film energy response

Energy response of Gafchromic EBT2 films to electrons was shown to be flat for electron energies between 6 and 20 MeV.[17] Since no data were available for energy response of the films to VHEE beams, we used MC simulations to predict the energy response of VHEE based on the work presented by Sutherland and Rogers.[18] Monoenergetic beams of 1–100 MeV and 1-cm FWHM were incident upon a sheet of Gafchromic EBT2 film placed on a 10 cm polystyrene phantom. The dose to the film D_{EBT2} was quantified by simulating the dose deposited in the film active layer. In order to evaluate the film energy response by means of D_{EBT2}/D_{water}, the dose with identical simulation setup but with the film material replaced with water D_{water} was modeled.

2.F. Dose rate independence of film

It has been demonstrated that Gafchromic EBT films were dose rate independent for irradiations with 20 MeV beams up to 1.5×10^{10} Gy/s.[19] With a pulse length of 1 ps, the maximum instantaneous dose rate on the film was expected to exceed this. We therefore performed a film dose rate independence study. A sheet of Gafchromic EBT2 film was placed at 4 mm depth in the polystyrene phantom that was positioned 8 cm away from the exit window. The dose per pulse was varied by setting the charge per pulse to 17.5, 25.3, and 53.0 pC. The phantom was irradiated with a 1 mm FWHM 60 MeV beam to a dose of 9 Gy using varying number of 1-ps long pulses to achieve the same dose at the film for each charge per pulse settings (Table II). The phantom was irradiated with 1–3 pulses for the 17.5, 25.3, and 53.0 pC beams, which resulted in 3.0×10^{12} to 9.0×10^{12} Gy/s dose rate/pulse, respectively. Three beams were delivered for each condition and the maximum doses per unit charge delivered to the film were quantified.

2.G. Absolute dosimetry

A number of sources of uncertainty affected the ability to model the absolute dose at the films, given the known beam parameters. Although charge per pulse was nominally known (at 30 pC), such low charge could only be measured with 10% accuracy. Additionally, with the experimental setup at the time, the charge could not be measured in real time and charge drifts due to the gun radio frequency phase and laser power drift could occur undetected during the experiment. Small apertures on the accelerating structures potentially scraped charge from the beam as it propagated through the beam line. Furthermore, the limited ability to control the beam size and shape at the time of the experiment may have been inconsistent with the modeling assumption of Gaussian beam profiles. As such, we anticipated a relatively large discrepancy in absolute dose of up to 50% between measurement and simulation.

We determined the differences in absolute dose between the film measurements at 0.64 cm depth and MC simulations to confirm that they fall within this range.

3. RESULTS

3.A. Comparison of experimental measurements and Monte Carlo simulations

The nominal beam parameters and measured FWHM on the film at 0.64 cm depth are summarized in Table I. The experimental and simulated PDD curves for all measured beams of both energies are shown in Fig. 2. The PDD_{exp}-PDD_{MC} difference curves in Fig. 2 demonstrate a good agreement between the experimental and simulation data with the largest discrepancy being 4%.

Relative beam profiles of experimental D_{exp} and simulated D_{MC} relative doses for all 50 and 70 MeV beams at four depths ranging from 6.4 to 74.6 mm along both major axes are shown in Figs. 3 and 4, respectively. Additionally, the dose difference $D_{exp} - D_{MC}$ is plotted. The results in Figs. 3 and 4 show that the dose difference was within 5% for all 50 and 70 MeV measured points.

3.B. VHEE beam spread due to the exit window, air, and uncertainty in beam energy and beam angular spread

As mentioned above, the beam FWHM at the accelerator exit window was back-calculated based on simulation data presented in Fig. 5(a). The relationship between input beam width and beam width at the phantom was found to be non-linear and highly energy dependent. The minimum beam FWHM at the film at 0.64 cm depth for an infinitesimally small input beam was calculated to be 4.0 and 3.0 mm for the 50 and 70 MeV beams, respectively.

Figure 5(b) summarizes the effects of beam energy and energy spread on central-axis depth dose curves of the largest 50 and 70 MeV beams. While the mean difference in dose due to energy measurement uncertainty was 2.8% and 2.5% for the 50 and 70 MeV beam, respectively, energy spread of 0.25% FWHM had a negligible effect on central-axis depth dose. The effect of the possible 0.286° beam angular spread resulted in mean dose difference of 2.5% and 1.4% for the 50 and 70 MeV beam, respectively.

3.C. Monte Carlo modeling of x-ray contamination due to exit window

The effect of x-ray contamination of the electron beam due to the presence of the steel exit window for 50 and 70 MeV beams is presented in Fig. 5(c). The contribution of x-ray dose to the total central-axis dose on the surface was approximately 1×10^{-2}% and 2×10^{-2}% of the maximum dose for the 50 and 70 MeV electron beam, respectively. Due to the greater attenuation of the electron beam, the relative x-ray dose contribution increased with depth. At 10 cm depth, the ratio of x-ray dose to total dose increased to 0.26% and 0.34% for the 50 and 70 MeV beam, respectively. X-ray contamination was higher for the 70 MeV beam compared to the 50 MeV beam due to the increasing bremsstrahlung cross-section with increasing electron beam energy.

3.D. EBT2 film energy response to electrons

The simulated energy response of EBT2 films for 1–100 MeV electrons plotted in Fig. 5(d) suggests that Gafchromic

T I. Beam parameters, measured and simulated doses at 0.64 cm depth.

Beam energy		50 MeV			70 MeV	
Nominal FWHM (mm)		5	3	2	3	1
Beam label		A	B	C	D	E
FWHM film @ 0.64 cm depth	x (mm)	7.3	5.8	5.5	4.4	4.0
	y (mm)	6.6	5.8	5.4	4.6	3.9
	Mean (mm)	6.9	5.8	5.4	4.5	4.0
Back-calculated FWHM	x (mm)	5.8	4.0	3.5	3.2	2.5
@ exit window	y (mm)	4.8	4.1	3.5	3.4	2.3
# of 30 pC (nominal) pulses		40	20	10	20	3
Measured dose (Gy)		2.87	3.03	1.20	6.29	1.08
Simulated dose (Gy)		4.06	2.73	1.54	4.67	0.95
Difference $(D_{MC} - D_{film})/D_{film}$ (%)		42	−10	28	−26	−12

T II. Measured doses by films as a function of dose rate for 60 MeV electron beams.

Dose rate (Gy/s)	Charge/pulse (pC)	# of pulses	Film dose (cGy/pC)	Diff. from mean (%)
3.0×10^{12}	17.5	3	17.2 ±0.5	−0.4
4.5×10^{12}	25.3	2	17.9 ±0.8	3.7
9.0×10^{12}	53.0	1	16.7 ±0.7	−3.3

EBT2 films have a flat, <2.5%, energy response in this energy range.

3.E. Dose rate independence of film

Table II summarizes the maximum doses per unit of charge measured with films for varying charge per pulse of 17.5, 25.3, and 53.0 pC to achieve a dose of 9 Gy, resulting in peak dose rates from 3.0×10^{12} to 9.0×10^{12} Gy/s. The results presented in the table show that Gafchromic EBT2 films are dose rate independent within 3.7% with 1 SD of 3.5% for peak dose rates between 3.0×10^{12} and 9.0×10^{12} Gy/s.

3.F. Uncertainty analysis

We have performed uncertainty analysis for MC simulations and experimental measurements of the presented relative dose deposition of VHEE beams in accordance with recommendations by the National Institute of Standards and Technology.[20] Table III summarizes the uncertainties and shows that the combined MC simulations uncertainty was estimated to be 4.7% and the experimental uncertainty was estimated to be 5.5% (both at 1 SD).

3.G. Absolute dosimetry

The differences in absolute dose between simulation and film measurement are summarized in Table I. MC doses differed from film doses by −26% to 42%, which are smaller discrepancies than expected based on known experimental uncertainties at the time. The largest MC dose overestimation of 42% for the largest 50 MeV beam (beam A) could be attributed to beam clipping.

4. DISCUSSION

The PDD curves in Fig. 2 show good agreement between simulation and experimental data for both energies. Central axis PDD at 8 cm depth ranged from 14% to 19% for the 5.4–6.9 mm 50 MeV beams and it ranged from 14% to 18% for the 4.0–4.5 mm 70 MeV beams. Additionally, beam profiles presented in Figs. 3 and 4 demonstrate how VHEE beam spatial spread increases with increasing depth.

The accuracy of MC simulations of the experimental setup was limited by a number of parameters that may have contributed to the observed differences with measurements. First, the beam FWHM at the exit window was not known and was back-calculated from the measurement of FWHM on the film at 0.64 cm depth. Second, zero beam angular spread was assumed in the primary simulations. In the experimental setup, however, the beams were kept focused using a set of quadrupole magnets and as a result, beam angular spread was possibly non-zero. Finally, beam energy spread could not be controlled easily and it was approximately 2%. The effects of beam angular spread and energy spread on the PDD of the largest beam for both energies were simulated and predicted to have a maximum 3%–3.8% discrepancy from simulations omitting these factors. In addition, as described above, several sources of experimental uncertainty in the absolute pulse charge and its propagation through the beam line predicted relatively large discrepancies in absolute dose.

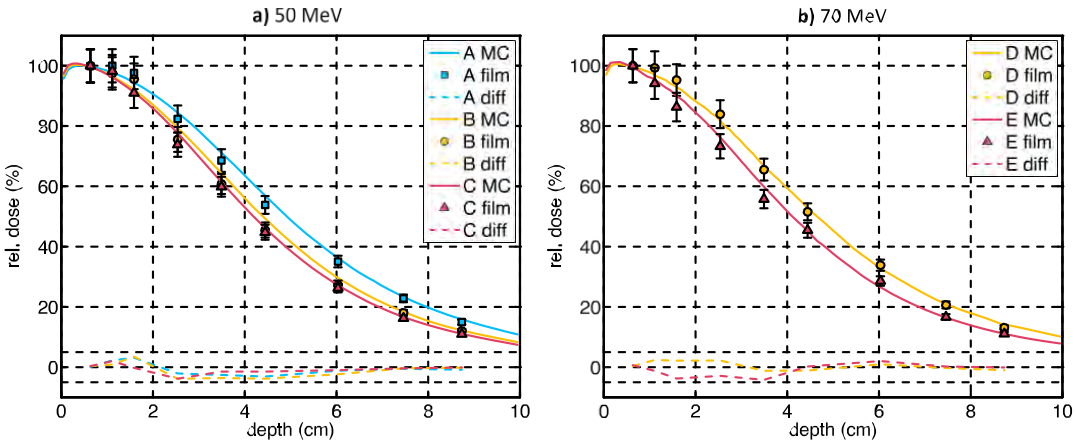

F . 2. Experimental (markers) and simulated (lines) PDD curves for 50 MeV (a) and 70 MeV (b) electron beams. FWHM in x and y of beams A-F are listed in Table I. Mean beam FWHMs are A: 6.9 mm, B: 5.8 mm, C: 5.4 mm, D: 4.5 mm, and E: 4.0 mm. PDD_{exp} – PDD_{MC} difference is also plotted and ±5% lines are shown for comparison purposes. All measurements agree well with simulations, with a maximum discrepancy of 4%.

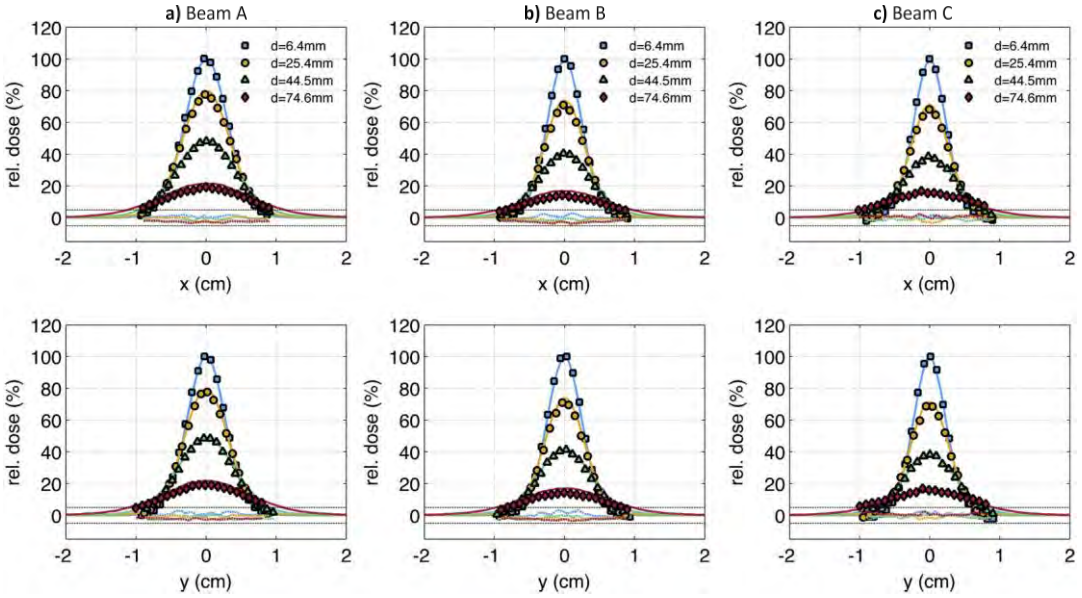

F . 3. Experimental (markers), simulated (solid lines), and difference (dashed) profiles for the three 50 MeV beams (A: 6.9 mm, B: 5.8 mm, C: 5.4 mm FWHM) plotted at four depths. The ±5% lines are shown for comparison purposes. All difference profiles fall between these lines.

Despite the uncertainties, agreement between relative dose Monte Carlo simulations and experiments was good, with maximum relative dose differences of 4% in percentage depth dose curves and 5% in beam profiles, even for absolute dosimetry, though substantial differences were smaller than anticipated.

In future experiments, we plan to measure the beam size at the exit window, the beam angular spread, the electron beam energy, and the pulse charge at the end of the beam line more accurately. We will consider using photoluminescence detector system imaging plates that have shown promise in absolute charge collection of 40 MeV electron beams delivered in tens of nC large and 2-ps long pulses.[23]

Neutron production in the phantom is mainly attributed to photonuclear reactions, which have two orders of magnitude higher probability than electronuclear reactions.[24] Based on work by DesRosiers *et al.*,[4] we estimated that neutron production in the polystyrene phantom accounted for 0.1% of total absorbed dose for the 70 MeV beam. The negligible neutron dose contribution justifies our choice of the EGSnrc MC code, which does not simulate neutron production and transport.

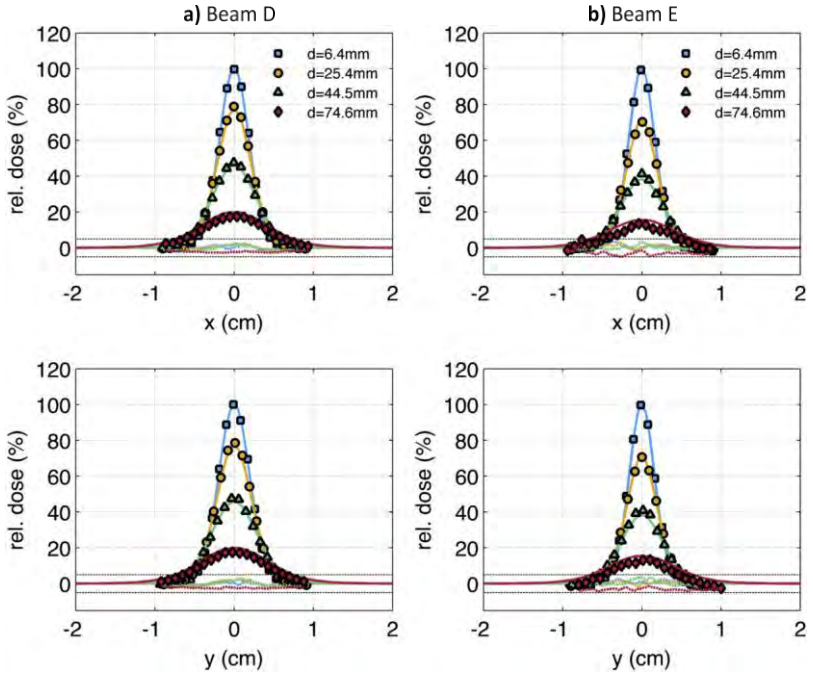

F . 4. Experimental (markers), simulated (solid lines), and difference (dashed) profiles for the two 70 MeV beams (D: 4.5 mm, and E: 4.0 mm FWHM) plotted at four depths. The ±5% lines are shown for comparison purposes. All difference profiles fall between these lines.

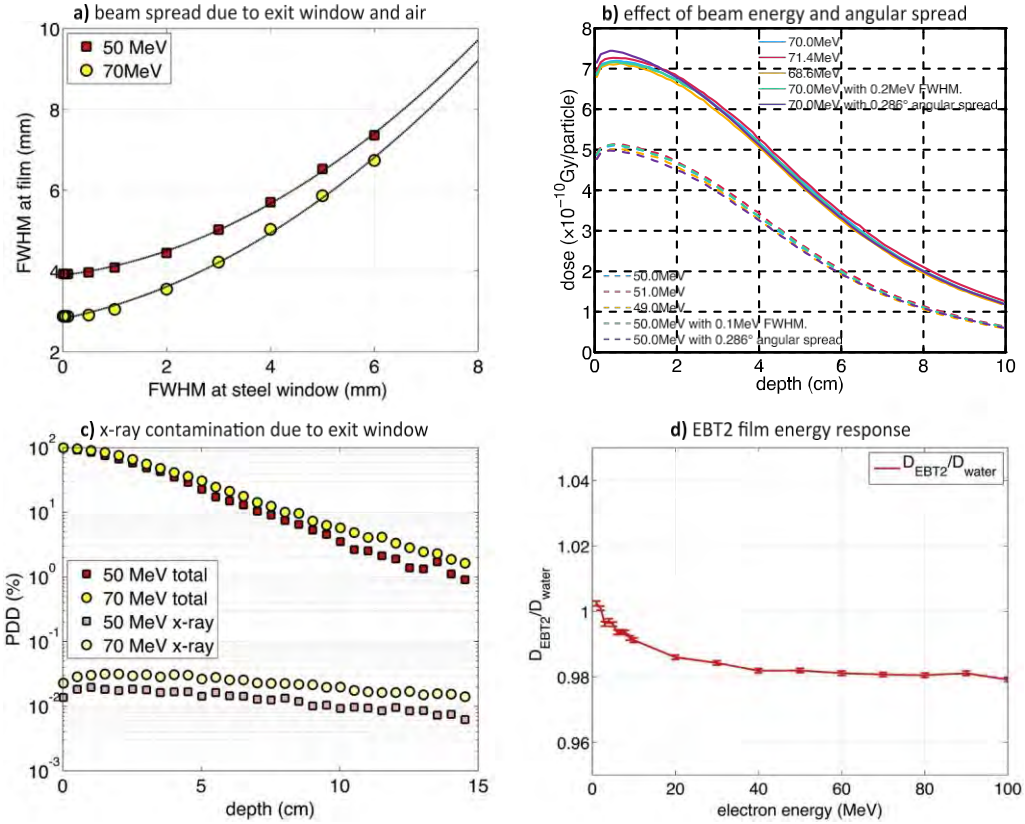

F . 5. Simulated beam spread due to exit window and air in the experimental setup, by which the beam FWHM at the exit window was back-calculated from measurements at the film at 0.64 cm depth (a). Simulated effects of beam energy and angular spread uncertainty on central-axis depth dose of the largest 50 and 70 MeV beams were small with a maximum impact of 3.8% due to the 0.286° angular spread (b). Simulated contribution of x-ray contamination generated by the steel window on 50 and 70 MeV PDDs was 2–4 orders of magnitude smaller than the total dose (c). Simulated Gafchromic EBT2 film energy response to electron beams was flat, with <1% change above 10 MeV (<2.5% above 1 MeV) (d).

5. CONCLUSIONS AND FUTURE WORK

Comparison of experimental homogeneous phantom relative dose measurements to EGSnrc Monte Carlo simulation for electron beam energies of 50 to 70 MeV showed agreement within 5% in terms of depth dose curves and beam profiles. Comparison of all 50 and 70 MeV beams showed absolute dose differences between measurements and simulations up to 42% and demonstrated the difficulties to accurately control and diagnose very high-energy electron beams delivered by a test linear accelerator. This critical issue that must be addressed before VHEE beams can be considered for clinical use. Further steps will include experimentally validating MC dose calculations in heterogeneous phantoms. This will confirm that the physics of VHEE interactions with matter is sufficiently well understood to be accurately modeled by MC methods, allowing us to use them for the design and planning of future high-energy electron radiation therapy systems. The MC model of the VHEE beam line will be used to calculate dose to samples in our future *in vitro* and *in vivo* studies of VHEE tumor and normal tissue radiobiology.

T III. Summary of relative dose MC simulation and experimental film measurement uncertainty estimates.

MC simulations (%)		Experiments (%)	
Statistical uncertainty	1.0	Film analysis (Ref. 21)	3.5
Stopping power (Ref. 22)	1.5	Film dose rate dependence	3.5
Energy spread	2.8	Film energy response	2.5
Beam angular spread	2.5		
Total	4.7	Total	5.5

ACKNOWLEDGMENTS

We would like to thank the NLCTA and SLAC Radiation Physics teams, particularly Juan Cruz, Carsten Hast, Matt Franzi, Jim Allen, and Henry Tran for adjusting the VHEE beam line, radiation measurements, and safety services during our experiments. We would also like to acknowledge support for this work from the Weston Havens Foundation, the Li Ka Shing Foundation, a Research Seed Grant from the American Association of Physicists in Medicine, a Stanford Bio-X Interdisciplinary Initiatives Program award, Stanford Department of Radiation Oncology, Stanford University School of Medicine, SLAC National Accelerator Laboratory, Stanford University Office of the Provost, the U.S. Department of Energy under Contract No. DE-AC02-76SF00515, and a U.S. Department of Defense Lung Cancer Research Program Idea Development Award No. W81XWH-12-LCRP-IDA. BWL, PGM, and ACK receive research support from Varian Medical Systems. BWL and PGM receive research support

from RaySearch Laboratories. BWL and PGM have received speaking honoraria from Varian Medical Systems.

[a]Present address: U.S. Department of Energy, Washington, DC.

[b]Authors to whom correspondence should be addressed. Electronic addresses: Peter.Maxim@Stanford.edu; Telephone: 650-725-4099; Fax: 650-498-5008 and BWLoo@Stanford.edu; Telephone: 650-736-7143; Fax: 650-725-8231.

[1]F. M. Khan and S. Stathakis, "The physics of radiation therapy," Med. Phys. **37**, 1374–1375 (2010).

[2]C. Griep, J. Davelaar, A. N. Scholten, A. Chin, and J. W.H. Leer, "Electron-beam therapy is not inferior to superficial x-ray therapy in the treatment of skin carcinoma," Int. J. Radiat. Oncol., Biol., Phys. **32**, 1347–1350 (1995).

[3]R. T. Hoppe, "Mycosis fungoides: Radiation therapy," Dermatol. Ther. **16**, 347–354 (2003).

[4]C. DesRosiers, V. Moskvin, A. F. Bielajew, and L. Papiez, "150-250 MeV electron beams in radiation therapy," Phys. Med. Biol. **45**, 1781–1805 (2000).

[5]L. Papiez, C. DesRosiers, and V. Moskvin, "Very high energy electrons (50-250 MeV) and radiation therapy," Technol. Cancer Res. Treat. **1**, 105–110 (2002).

[6]C. Yeboah, G. A. Sandison, and V. Moskvin, "Optimization of intensity-modulated very high energy (50–250 MeV) electron therapy," Phys. Med. Biol. **47**, 1285–1301 (2002).

[7]C. Yeboah and G. A. Sandison, "Optimized treatment planning for prostate cancer comparing IMPT, VHEET and 15 MV IMXT," Phys. Med. Biol. **47**, 2247–2261 (2002).

[8]V. Moskvin, F. Salvat, D. K. Stewart, and C. M. DesRosiers, "Monte Carlo engine for treatment planning in radiation therapy with very high energy electrons (VHEE) of 150-250 MeV," *IEEE Nuclear Science Symposium and Medical Imaging Conference (2010 NSS/MIC)* (IEEE, New York, NY, 2010).

[9]J. Baro, J. Sempau, J. M. Fernandezvarea, and F. Salvat, "PENELOPE - An algorithm for Monte-Carlo simulation of the penetration and energy-loss of electrons and positrons in matter," Nucl. Instrum. Methods Phys. Res., Sect. B **100**, 31–46 (1995).

[10]I. J. Chetty, J. M. Moran, T. S. Nurushev, D. L. McShan, B. A. Fraass, S. J. Wilderman, and A. F. Bielajew, "Experimental validation of the DPM Monte Carlo code using minimally scattered electron beams in heterogeneous media," Phys. Med. Biol. **47**, 1837–1851 (2002).

[11]I. J. Chetty, J. M. Moran, D. L. McShan, B. A. Fraass, S. J. Wilderman, and A. F. Bielajew, "Benchmarking of the dose planning method (DPM) Monte Carlo code using electron beams from a racetrack microtron," Med. Phys. **29**, 1035–1041 (2002).

[12]A. Brahme, T. Kraepelien, and H. Svensson, "Electron and photon beams from a 50 MeV racetrack microtron," Acta Oncol. **19**, 305–319 (1980).

[13]I. Kawrakow and D. W. O. Rogers, "The EGSnrc code system: Monte Carlo simulation of electron and photon transport," NRCC (2006).

[14]M. Dunning, C. Adolphsen, T. S. Chu, E. Colby, S. Gilevich, C. Hast, K. Jobe, C. G. Limborg-Deprey, D. McCormick, and B. D. McKee, "Status and upgrade of NLCTA for studies of advanced beam acceleration, dynamics and manipulations," Energy **100**, 130–132 (2011).

[15]D. W. O. Rogers, B. A. Faddegon, G. X. Ding, C. M. Ma, J. We, and T. R. Mackie, "BEAM - A Monte-Carlo code to simulate radiotherapy treatment units," Med. Phys. **22**, 503–524(1995).

[16]B. R. B. Walters, I. Kawrakow, and D. W. O. Rogers, DOSXYZnrc users manual, NRCC, 2007.

[17]B. Arjomandy, R. Tailor, A. Anand, N. Sahoo, M. Gillin, K. Prado, and M. Vicic, "Energy dependence and dose response of Gafchromic EBT2 film over a wide range of photon, electron, and proton beam energies," Med. Phys. **37**, 1942–1947 (2010).

[18]J. G. H. Sutherland and D. W.O. Rogers, "Monte Carlo calculated absorbed-dose energy dependence of EBT and EBT2 film," Med. Phys. **37**, 1110–1116 (2010).

[19]L. Karsch, E. Beyreuther, T. Burris-Mog, S. Kraft, C. Richter, K. Zeil, and J. Pawelke, "Dose rate dependence for different dosimeters and detectors: TLD, OSL, EBT films, and diamond detectors," Med. Phys. **39**, 2447–2455 (2012).

[20]B. N. Taylor and C. E. Kuyatt, NIST technical note 1297, Guidelines for evaluating and expressing the uncertainty of NIST measurement results, 1994.

[21]S. Devic, J. Seuntjens, E. Sham, E. B. Podgorsak, C. R. Schmidtlein, A. S. Kirov, and C. G. Soares, "Precise radiochromic film dosimetry using a flat-bed document scanner," Med. Phys. **32**, 2245–2253 (2005).

[22]ICRU, "Stopping powers for electrons and positrons," ICRU Report No. 37 (ICRU, Bethesda, MD, 1984).

[23]K. Zeil, S. D. Kraft, A. Jochmann, F. Kroll, W. Jahr, U. Schramm, L. Karsch, J. Pawelke, B. Hidding, and G. Pretzler, "Absolute response of Fuji imaging plate detectors to picosecond-electron bunches," Rev. Sci. Instrum. **81**, 013307 (2010).

[24]ICRU, "Electron beams with energies between 1 and 50 MeV," ICRU Report No. 35 (ICRU, Bethesda, MD, 1984).

Treatment planning for radiotherapy with very high-energy electron beams and comparison of VHEE and VMAT plans

Magdalena Bazalova-Carter, Bradley Qu, and Bianey Palma
Department of Radiation Oncology, Stanford University, Stanford, California 94305

Björn Hårdemark and Elin Hynning
RaySearch Laboratories AB, Stockholm SE-103 65, Sweden

Christopher Jensen, Peter G. Maxim,[a] and Billy W. Loo, Jr.[a]
Department of Radiation Oncology, Stanford University, Stanford, California 94305

(Received 22 December 2014; revised 7 April 2015; accepted for publication 12 April 2015; published 29 April 2015)

Purpose: The aim of this work was to develop a treatment planning workflow for rapid radiotherapy delivered with very high-energy electron (VHEE) scanning pencil beams of 60–120 MeV and to study VHEE plans as a function of VHEE treatment parameters. Additionally, VHEE plans were compared to clinical state-of-the-art volumetric modulated arc therapy (VMAT) photon plans for three cases.
Methods: VHEE radiotherapy treatment planning was performed by linking EGSnrc Monte Carlo (MC) dose calculations with inverse treatment planning in a research version of RayStation. In order to study the effect of VHEE treatment parameters on VHEE dose distributions, a graphical user interface (GUI) for calculation of VHEE MC pencil beam doses was developed. Through the GUI, pediatric case MC simulations were run for a number of beam energies (60, 80, 100, and 120 MeV), number of beams (13, 17, and 36), pencil beam spot (0.1, 1.0, and 3.0 mm) and grid (2.0, 2.5, and 3.5 mm) sizes, and source-to-axis distance, SAD (40 and 50 cm). VHEE plans for the pediatric case calculated with the different treatment parameters were optimized and compared. Furthermore, 100 MeV VHEE plans for the pediatric case, a lung, and a prostate case were calculated and compared to the clinically delivered VMAT plans. All plans were normalized such that the 100% isodose line covered 95% of the target volume.
Results: VHEE beam energy had the largest effect on the quality of dose distributions of the pediatric case. For the same target dose, the mean doses to organs at risk (OARs) decreased by 5%–16% when planned with 100 MeV compared to 60 MeV, but there was no further improvement in the 120 MeV plan. VHEE plans calculated with 36 beams outperformed plans calculated with 13 and 17 beams, but to a more modest degree (<8%). While pencil beam spacing and SAD had a small effect on VHEE dose distributions, 0.1–3 mm pencil beam sizes resulted in identical dose distributions. For the 100 MeV VHEE pediatric plan, OAR doses were up to 70% lower and the integral dose was 33% lower for VHEE compared to 6 MV VMAT. Additionally, VHEE conformity indices (CI_{100} = 1.09 and CI_{50} = 4.07) were better than VMAT conformity indices (CI_{100} = 1.30 and CI_{50} = 6.81). The 100 MeV VHEE lung plan resulted in mean dose decrease to all OARs by up to 27% for the same target coverage compared to the clinical 6 MV flattening filter-free (FFF) VMAT plan. The 100 MeV prostate plan resulted in 3% mean dose increase to the penile bulb and the urethra, but all other OAR mean doses were lower compared to the 15 MV VMAT plan. The lung case CI_{100} and CI_{50} conformity indices were 3% and 8% lower, respectively, in the VHEE plan compared to the VMAT plan. The prostate case CI_{100} and CI_{50} conformity indices were 1% higher and 8% lower, respectively, in the VHEE plan compared to the VMAT plan.
Conclusions: The authors have developed a treatment planning workflow for MC dose calculation of pencil beams and optimization for treatment planning of VHEE radiotherapy. The authors have demonstrated that VHEE plans resulted in similar or superior dose distributions for pediatric, lung, and prostate cases compared to clinical VMAT plans.[http://dx.doi.org/10.1118/1.4918923]

Key words: very high-energy electrons, Monte Carlo, treatment planning, pediatric patient, integral dose

1. INTRODUCTION

Deep-seated tumors are typically treated with 6–15 MV photon beams delivered by medical linear accelerators. Previous work has demonstrated in principle dosimetric advantages of using very high-energy (50–250 MeV) electron (VHEE) beams for radiation therapy of deep-seated tumors.[1–4] Monte Carlo (MC) simulations with the code showed that electron beams of such high energies have similar to superior dose deposition properties compared to currently clinically

used photon beams. For example, intensity-modulated VHEE therapy for prostate cancer at 250 MeV energy outperformed intensity-modulated radiation therapy (IMRT) with 15 MV photon beams.[4]

VHEE plans are not only superior to IMRT plans, but they can be delivered by orders of magnitude faster than photon plans mainly due to three effects. (1) X-ray beam production in the head of a linear accelerator has an approximately 3% efficiency [6% in flattening filter free (FFF) mode].[5] (2) Lower number of electrons compared to photons is needed to deliver the same dose (discussed in this work). (3) Unlike photon beams that are delivered from multiple angles by means of gantry rotation, electron beams can be steered electromagnetically, which can be done in the order of milliseconds. In summary, while treatment delivery of stereotactic doses of more than 15 Gy with photon beams typically lasts 2–10 min, treatments with VHEE beams for the same dose can be in principle delivered within seconds.

We have proposed a conceptual design of a VHEE treatment machine with a compact electron accelerator to deliver radiotherapy with a VHEE scanning pencil beam.[6] In order to capitalize on the potential speed advantages of VHEE, the design should minimize the need for mechanical motion. An approach to directing beams to the patient from multiple angles without a rotating gantry would be to have multiple fixed beam lines (e.g., 10–30) arrayed around the patient. These beam lines could each have a VHEE Linac, or share a common VHEE Linac whose beam is sequentially directed to each of the beam lines in rapid succession. A pencil beam from each of the beam lines, potentially with electronically adjustable size, would be rapidly raster-scanned over an area covering the beam's-eye projection of the target region to produce intensity-modulated fields from each beam direction. A high-efficiency and high-gradient Linac design[7] would be required for the system to fit in existing radiation therapy vaults. There would be a compromise between the space required to accelerate and steer the beam toward the patient, and the bore size or clearance around the patient, which should be at a minimum equal to or larger than the bore size of scanners used for radiation therapy simulation (e.g., 70 cm or larger). Therefore, the minimum distance from the end of the electron beamline to the isocenter of the system should be 40–50 cm (accounting for additional space required for beam measurement and diagnostic systems that might need to be in the beam path).

In this paper, we present a workflow for treatment planning for intensity-modulated scanning VHEE pencil beam therapy. We demonstrate that VHEE dose distributions for a pediatric, lung, and prostate case are superior or similar to state-of-the-art volumetric modulated arc therapy (VMAT) dose distributions.

2. MATERIALS AND METHODS

A treatment-planning tool for radiotherapy with VHEE scanning beam has been developed by linking MC pencil beam dose calculations with a commercially available treatment planning system. Specifically, VHEE pencil beam dose was calculated in the EGSnrc MC codes (V4 2.4.0)[8] and imported into a research version of RayStation (version 4.4.100.0, RaySearch Laboratories AB, Stockholm, Sweden) for treatment planning optimization (Fig. 1). To facilitate treatment planning for a large number of cases and VHEE treatment parameters, a [redacted] (version R2010b, The Mathworks, Natick, MA) GUI was developed.

VHEE pencil beam MC dose calculations, the [redacted] GUI, and the entire treatment planning process are described in Secs. 2.A–2.C. Additionally, three clinical cases are described. In one case (a pediatric brain tumor treatment plan), VHEE planning parameters, including beam energy, number

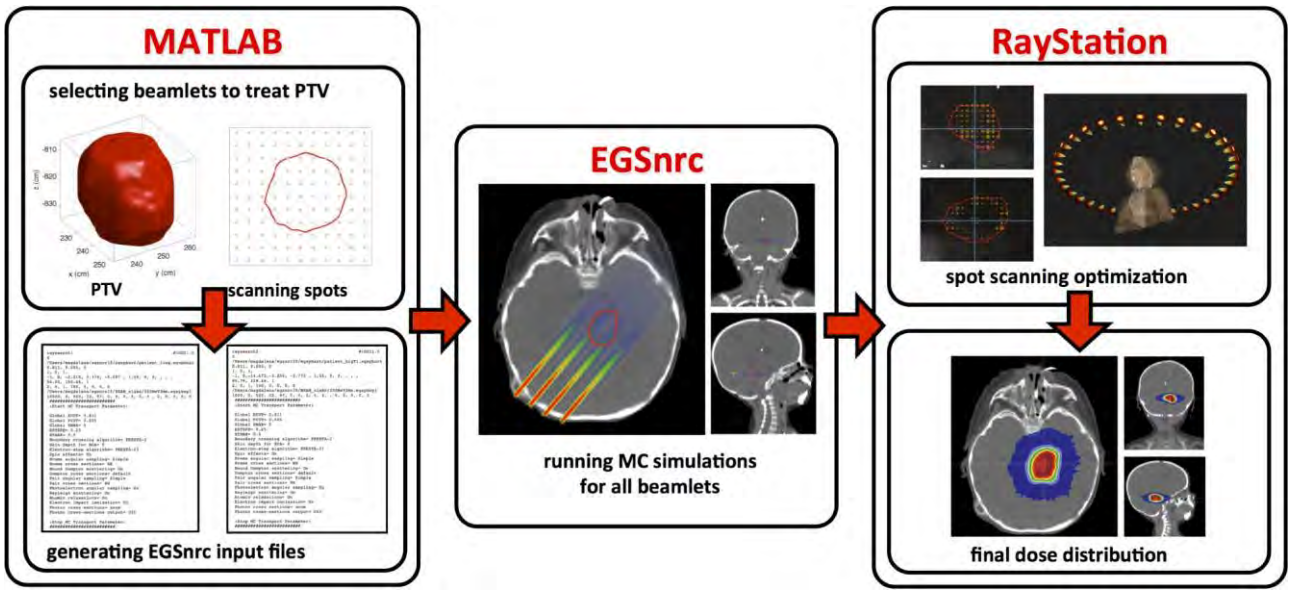

FIG. 1. Workflow diagram for VHEE scanning beam treatment planning. EGSnrc MC input files are generated in [redacted], MC pencil beam doses are calculated in EGSnrc, and final VHEE dose distribution is optimized in RayStation.

T I. Tissue assignment table.

	Air	Lung	Soft tissue	Cortical bone	Metal
HU range	< − 950	[−950; −300]	[−300; 300]	[300; 3094]	>3094

of beam angles, source-to-axis distance, and pencil beam size and spacing, were varied in order to determine the optimal configuration. For all three cases, VHEE and VMAT plan comparisons are presented.

2.A. Monte Carlo dose calculations

2.A.1. Pencil beam generation

BEAMnrc (V4 2.4.0)[9] was used to simulate VHEE pencil beams of 60–120 MeV and sizes of 0.1–5 mm defined by the full width at half maximum (FWHM). Monoenergetic beams with Gaussian distributions in x and y directions (ISOURCE = 19) were used as the source of electrons. The VHEE phase–space files collected below a 0.1-mm thin air layer were used for patient dose calculations in the DOSXYZnrc MC code.[10] Note that VHEE beams traversed an air gap of 30–45 cm before being incident on the patient skin. No accelerator exit window and parallel beams were modeled throughout this work. However, we confirmed that a thin 50-μm beryllium exit window had a negligible effect on the quality of the calculated VHEE dose distributions for targets >2 cm. Note that we reported a 5% agreement between measured and EGSnrc-calculated dose deposited by 50–70 MeV electron beams.[11]

2.A.2. Patient-specific anatomy

Patient CT images were first cropped around the body structure with a 10 mm margin, down sampled to voxel size of 1.5–5 mm and converted into .egsphant MC anatomy files using the piece-wise linear CT number-to-mass density calibration curve of our GE Discovery ST multislice PET/CT scanner (GE Medical Systems, Waukesha, WI). While the region outside of body contour was assigned to air, four tissue types and metal were used for tissue assignment inside the body structure. The tissue assignment was done based on HU ranges listed in Table I.

2.A.3. Pencil beam dose calculations

For each beam angle, the projection of the target structure was found using Radon transform[12] and the rectangle bounding the target to be filled with pencil beam aiming spots was identified (Fig. 2). The coordinates of pencil beam aiming spots were calculated based on the selected beam angle and pencil beam spacing. The DOSXYZnrc VHEE phase–space source θ and ϕ polar angles for ISOURCE = 8 were determined based on the pencil beam aiming spot coordinates and the source-to-axis/isocenter distance (SAD). For each VHEE pencil beam simulation, 5×10^3 electrons were modeled resulting in statistical uncertainty of less than 2% along the pencil beam path. The overall statistical uncertainty of VHEE dose distributions in high dose regions was 0.1%–0.4%. All interactions of electrons and photons, including triplet production, photonuclear attenuation, radiative Compton correction, electron impact ionization, and Rayleigh scattering, were included in the simulations. The National Institute of Standards and Technology (NIST) XCOM cross-section database[13] was selected. Electrons and photons were tracked down to kinetic energies of 100 and 10 keV, respectively.

2.B. matlab GUI

In order to facilitate VHEE treatment planning in a user-friendly fashion, a GUI for pencil beam MC dose calculations was written and is described in Sec. 2.B.1.

2.B.1. User input

First, patient CT images with the DICOM structure file were loaded in the GUI (Fig. 3) and the target structure to be treated was chosen. Subsequently, VHEE treatment-planning parameters summarized in Table II, such as the electron beam energy, pencil beam size and spacing, and the number of uniformly distributed beams over a full arc, were selected. SADs of 40 and 50 cm were evaluated to correspond to practical bore sizes of a machine designed to fit into conventional treatment vaults with adequate room for high-energy Linacs and sufficient clearance around a patient. MC pencil beam dose calculations for the selected parameters

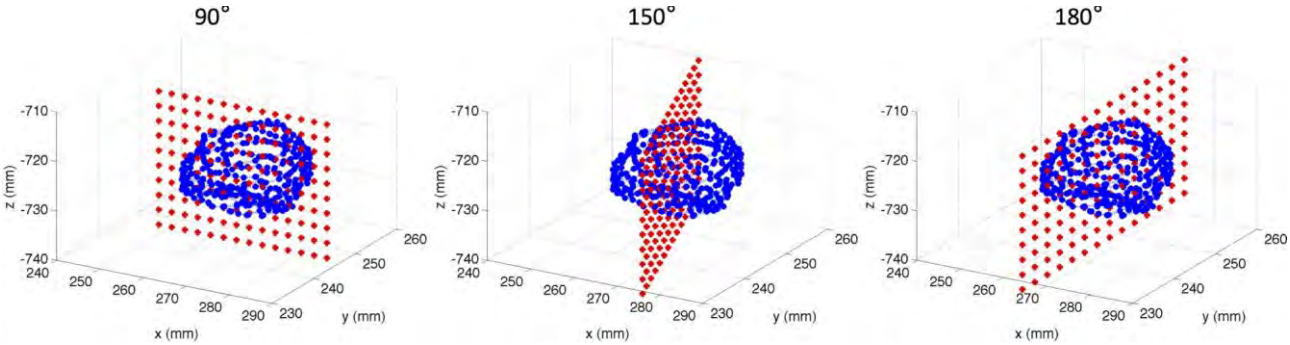

F . 2. Pencil beam aiming spots (crosses) spaced by 3 mm at 90°, 150°, and 180° beam angles for the pediatric patient brain target (circles) optimized for VHEE radiotherapy in this work.

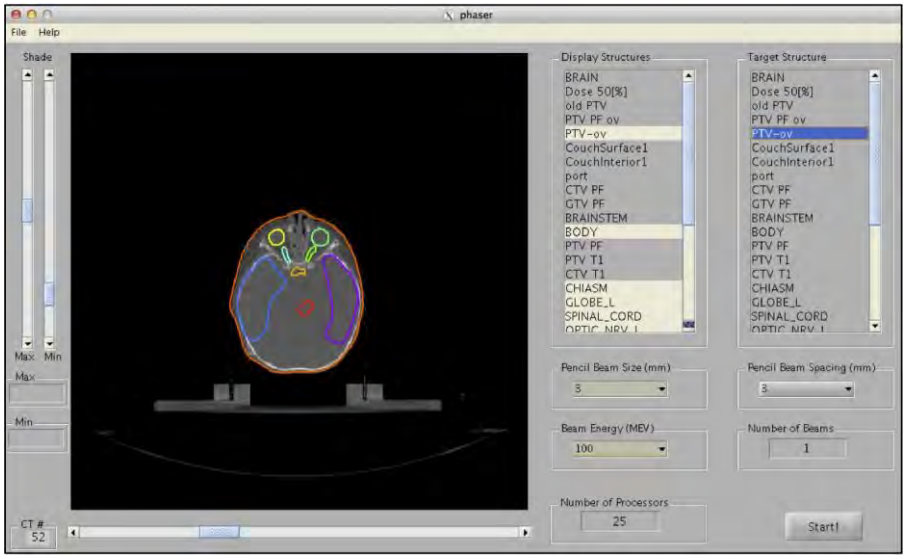

F . 3. GUI for MC calculation of VHEE pencil beams.

were then launched on a specified number of processors of a 16 × 3 GHz Quad-Core Intel Xeon computer. As a result, a compressed file containing sparse matrices with VHEE pencil beam doses importable into RayStation was generated.

2.B.2. Monte Carlo dose calculation flowchart

The flowchart of the GUI processes is presented in Fig. 4. In the first step, in order to save calculation time, the existence of the patient's anatomy .egsphant file and the pencil beam phase–space file with the selected beam size and energy was verified [Fig. 4(a)]. If the .egsphant and the phase–space files did not exist, the GUI generated the files as described in Sec. 2.A.2.

In the second step, DOSXYZnrc input files for all N beams of the plan were generated and run on a beam per beam basis [Fig. 4(b)]. Each nth beam ($n = 1, 2, \ldots, N$) was composed of M_n pencil beams arranged in a rectangular grid (Fig. 2). MC pencil beam dose calculations were run in parallel using the specified number of processors. Since most of the dose matrix elements were zeros, pencil beam dose data were made sparse in order to save hard-disk space. After the completion of MC pencil beam dose calculations for each beam, pencil beam data were resorted to match RayStation format.

Additionally, a RayStation header file with pencil beam information for each beam of the plan was generated. The header file contained general information about the pencil beam MC dose calculations, such as the dose grid dimensions, its location, and the dose calculation voxel size. For each beam, the beam gantry angle, its isocenter and pencil beam grid, and location together with the MC pencil beam data file name were also listed. Finally, an output text file with plan information containing the selected treatment parameters was created.

2.C. Treatment planning optimization

Spot-scanning inverse treatment planning was performed in a research version of RayStation with a modified version of RayStation's proton pencil beam scanning optimization algorithm.[14] For each plan, MC-simulated pencil beams and the GUI-generated header file were imported into RayStation, and RayStation beam setup was generated with a (version 2.7.1) script using the header file. More specifically, the beam angles and isocenters, the dose calculation grid, and the pencil beam aiming spots with respect to the beam isocenter were specified.

Target and organ-at-risk (OAR) dose objectives for each of the studies cases were determined based on the dose volume histograms (DVHs) of the clinical treatment plans. Once the objectives were satisfied, the dose to normal tissues was decreased within the limits of each VHEE plan.

T II. Plan parameters for VHEE treatment parameter study applied on a pediatric patient.

Studied parameter	Energy (MeV)	Number of beams	SAD (cm)	Pencil beam size (mm)	Pencil beam spacing (mm)
Energy	60, 80, 100, 120	13	40	1.0	2.5
Number of beams	80	13, 17, 36	40	1.0	2.5
SAD	80	13	40, 50	1.0	2.5
Pencil beam size	80	13	40	0.1, 1.0, 3.0	2.5
Pencil beam spacing	80	13	40	1.0	2.0, 2.5, 3.5

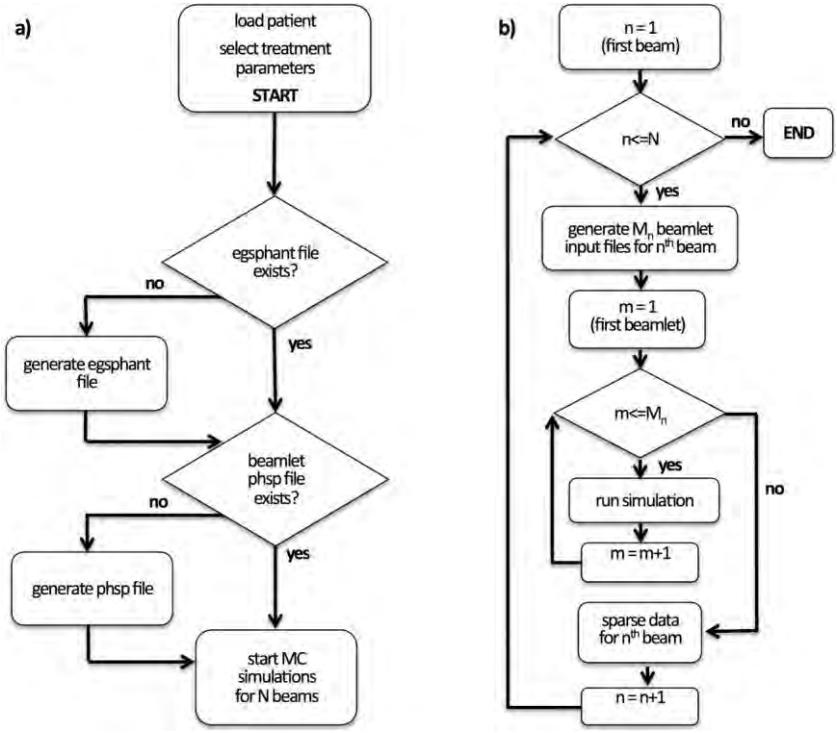

F . 4. GUI MC pencil beam dose calculation flowchart for phantom and phase–space file generation (a) and MC pencil beam dose calculations (b).

VHEE treatment plans for a number of treatment parameters (Table II) were then compared to each other and to the clinical plans.

2.D. Cases

The presented workflow for VHEE treatment planning is demonstrated on a pediatric, lung, and prostate case. 100 MeV VHEE plans for all three cases were compared to the clinical VMAT plans by means of dose difference maps, DVHs, and conformity indices CI_{100} and CI_{50}. Conformity index CI_x was calculated with

$$CI_x = \frac{V_x}{V_{PTV}}, \quad (1)$$

where V_x is the volume encompassed by x% of the prescription dose and V_{PTV} is the planning target volume (PTV) volume. All VHEE plans were normalized such that the 100% isodose line covered 95% of the target volume. The cases studied in this work are briefly described in Secs. 2.D.1–2.D.3 and their VHEE treatment planning parameters are summarized in Table III.

2.D.1. Pediatric case

The patient's 4 cm^3 PTV wrapped around the brainstem was clinically treated with a single-arc 6 MV VMAT. The prescription dose to the target was 3620 cGy to 95% volume. The pediatric patient was planned with VHEE beams using combinations of treatment parameters summarized in Table II. For each of the studied treatment planning parameters, the other parameters were kept at default values (80 MeV, 13 beams, 40 cm SAD, 1 mm pencil beam size, and 2.5 mm spacing). The mean doses to four OARs with the highest mean dose (the brainstem, chiasm, and left and right temporal lobes) were quantified. A 100 MeV VHEE plan was also compared to the clinical VMAT plan using treatment parameters summarized in Table III.

The VHEE MC dose calculation grid consisted of 170 × 130 × 85 voxels with (1.8 × 1.8 × 4.0) mm^3 in size. The number of calculated beamlets per beam varied from 80 for the 3.5 mm

T III. VHEE treatment planning parameters for VMAT comparison for three cases.

	Energy (MeV)	Number of beams	SAD (cm)	Pencil beam size (mm)	Pencil beam spacing (mm)
Pediatric case	100	36	40	1.0	2.0
Lung case	100	36	50	2.0	2.0
Prostate case	100	36	50	3.0	3.0

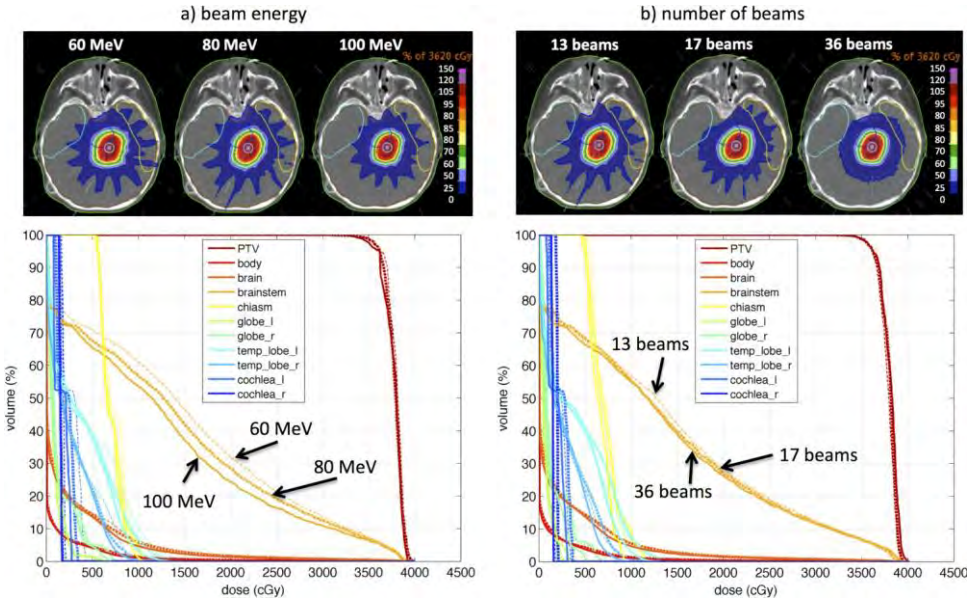

F . 5. Pediatric case VHEE DVHs and dose distributions as a function of beam energy (60 MeV: dashed–dotted, 80 MeV: dashed, 100 MeV: solid) for plans with 13 beams (a) and as a function of number of beams (13: dash-dotted, 17: dashed, 36: solid) for plans with 80 MeV (b).

pencil beam spacing to 364 for 2.0 mm pencil beam spacing. MC dose calculations of the entire plan lasted from 1 to 36 h using 50 CPUs.

2.D.2. *Lung case*

The lung case with a 66 cm^3 PTV in the right lung was clinically treated with a single-arc 6 MV FFF VMAT to a prescription dose of 5000 cGy to 95% PTV. The case was planned with VHEE parameters listed in Table III. The VHEE MC dose calculation grid consisted of 161 × 86 × 84 voxels with (2.9 × 2.9 × 5.0) mm^3 in size. The number of calculated beamlets per beam was on average 1600 and MC dose calculation of the entire plan took approximately 36 h using 50 CPUs.

2.D.3. *Prostate case*

The prostate case with a 113 cm^3 PTV was planned with VHEE using parameters listed in Table III. Clinically, the prostate case was treated with two-arc 15 MV VMAT to a dose of 7800 cGy to 95% PTV. The VHEE MC dose calculation grid consisted of 125 × 84 × 89 voxels with (3.3 × 3.3 × 3.7) mm^3 in size. The number of calculated beamlets per beam was on average 600 and MC dose calculation of the entire plan took approximately 20 h using 50 CPUs.

3. RESULTS

Pediatric case VHEE treatment plans as a function of studied treatment parameters are described in Sec. 3.A. Additionally, 100 MeV pediatric, lung and prostate VHEE plans are compared to the clinically delivered VMAT plans.

3.A. Parameter study

The results of the treatment parameter study performed on the pediatric patient are summarized in Fig. 5. VHEE beam energy and the number of beams had the largest effect on the quality of dose distributions. The dose falloff outside of the target increased and OAR doses decreased with increasing beam energy up to 100 MeV and with increasing the number of beams. The mean doses to the brainstem, chiasm, and left and right temporal lobes are summarized in Table IV.

Compared to the 60 MeV plan, the 100 MeV mean doses to the left and right temporal lobe, the brainstem, and the chiasm were decreased by 16%, 13%, 13%, and 5%, respectively. The

T IV. Mean doses (in cGy) to four pediatric case OARs with the highest dose as a function of VHEE beam energy and number of beams.

	Energy (MeV)				Number of beams		
	60	80	100	120	13	17	36
Brainstem	1456	1359	1262	1306	1359	1332	1303
Chiasm	736	709	697	735	709	706	652
Left temporal lobe	425	392	356	340	392	390	365
Right temporal lobe	282	256	245	233	256	255	246

T V. PTV volume and prescription dose, VHEE plan calculation parameters, and conformity indices for the studied clinical cases.

Case	PTV volume (cm^3)	Prescription dose (cGy)	Number of pencil beams	Pencil beam spacing (mm)	Number of electrons	CI_{100}		CI_{50}	
						VHEE	VMAT	VHEE	VMAT
Pediatric	4	3620	9 200	2.0	5.76×10^{11}	1.09	1.30	4.07	6.81
Lung	66	5000	49 000	2.0	6.17×10^{12}	1.09	1.12	4.05	4.39
Prostate	113	7800	21 900	3.0	1.25×10^{13}	1.04	1.03	4.73	4.99

120 MeV plan with increased mean dose to the brainstem and chiasm did not outperform the 100 MeV plan. The number of beams affected the OAR doses to a lesser extent, with the largest dose differences between the 13- and 36-beam plan to the chiasm (8%) and the left temporal lobe (7%). Mean dose differences to the other OARs for these two studied parameters were within 4%.

While SAD and pencil beam spacing had a minor effect on dose distributions with OAR dose differences <5%, the studied pencil beam sizes generated nearly identical treatment plans with negligible differences in OAR doses.

3.B. Comparison to VMAT plans

Sections 3.B.1–3.B.3 describe comparison of 100 MeV VHEE plans to the clinical VMAT plans for the pediatric, lung, and prostate cases. Quantitative results are summarized in Table V.

3.B.1. Pediatric case

The VHEE plan calculated based on the studied parameters with the lowest OAR doses was identified as the plan with 100 MeV 1 mm pencil beams spaced by 2 mm delivered with 36 beams and 40 cm SAD. Figure 6 presents a comparison of the 100 MeV pediatric VHEE plan with the clinical 6 MV VMAT plan by means of dose distributions and dose differences in an axial and coronal slice, by means of DVHs and OAR mean doses.

As seen in Fig. 6, the VHEE dose was tighter around the target compared to the VMAT dose, which is also reflected by the 33% decrease in integral dose. The mean dose to

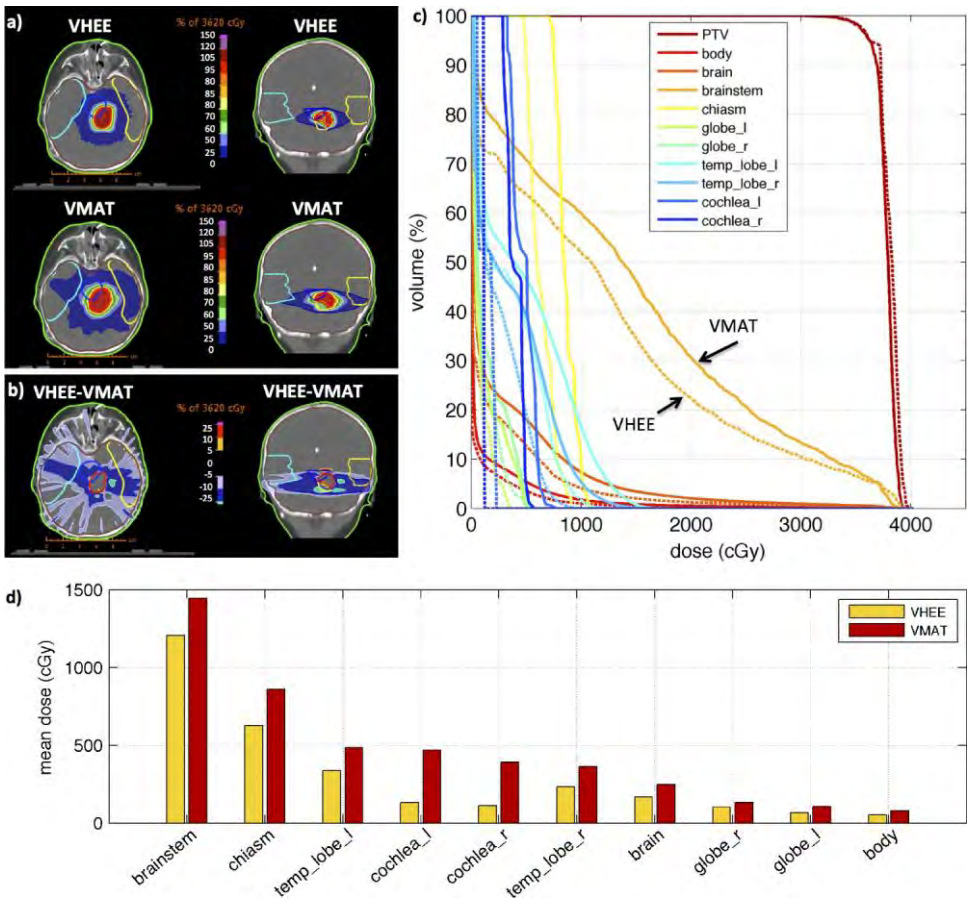

F . 6. Pediatric case dose distributions (a), dose difference maps (b), DVHs (c), and organ mean doses (d) for the best VHEE plan and the clinical 6 MV VMAT plan.

both cochleae is decreased by up to 70% in the VHEE plan compared to the VMAT plan. Additionally, the VHEE mean dose to both temporal lobes is more than 30% lower than the VMAT dose. In summary, all VHEE OAR mean doses were lower than VMAT OAR mean doses.

Additionally, the VHEE plan (CI_{100} = 1.09) was more conformal than the VMAT plan (CI_{100} = 1.30). The integral dose savings of the VHEE plan were reflected by the significantly lower CI_{50} = 4.07 compared to the VMAT plan with CI_{50} = 6.81. The 100 MeV VHEE plan for the pediatric case consisted of 9200 pencil beams with nonzero weights. The plan required 5.76×10^{11} electrons to deliver the entire treatment dose of 3620 cGy.

3.B.2. Lung case

The lung case dose distributions, DVHs, and mean OAR doses for the 100 MeV VHEE plan and the clinically delivered VMAT plan are presented in Fig. 7. All OARs received lower mean doses in the VHEE plan compared to the VMAT plan, with maximum OAR sparing for the left lung (27%) and body, esophagus, and chest wall (all 19%). Additionally, the VHEE CI_{100} = 1.09 and CI_{50} = 4.05 were lower than the CI_{100} = 1.12 and CI_{50} = 4.39 of the VMAT plan reflecting a higher conformality of the VHEE plan compared to the VMAT plan. The lung plan consisted of 49 000 nonzero weight pencil beams with a total of 6.17×10^{12} electrons to deliver the entire treatment dose of 5000 cGy.

3.B.3. Prostate case

The prostate case dose distributions, DVHs, and mean OAR doses for the 100 MeV VHEE plan, and the clinically delivered VMAT plan are presented in Fig. 8. The VHEE mean doses to the urethra and the penile bulb were 3% higher and the VHEE dose to the rectum was 3% lower compared to the VMAT plan. The VHEE mean dose to all the other OARs was by 14%–84% lower than in the VMAT plan. While the CI_{100} was slightly higher in the VHEE plan (1.04) than in the VMAT plan (1.03), CI_{50} was lower in the VHEE plan (4.73) compared to the VMAT plan (4.99). The VHEE plan consisted of 21 900 nonzero weight pencil beams with a total of 1.25×10^{13} electrons to deliver the entire treatment dose of 7800 cGy.

4. DISCUSSION

We have presented a treatment planning workflow for radiotherapy with very high-energy electron beams. We have demonstrated that 100 MeV VHEE dose distribution for a pediatric brain case and a lung case outperformed the clinical state-of-the-art VMAT plans and that 100 MeV prostate

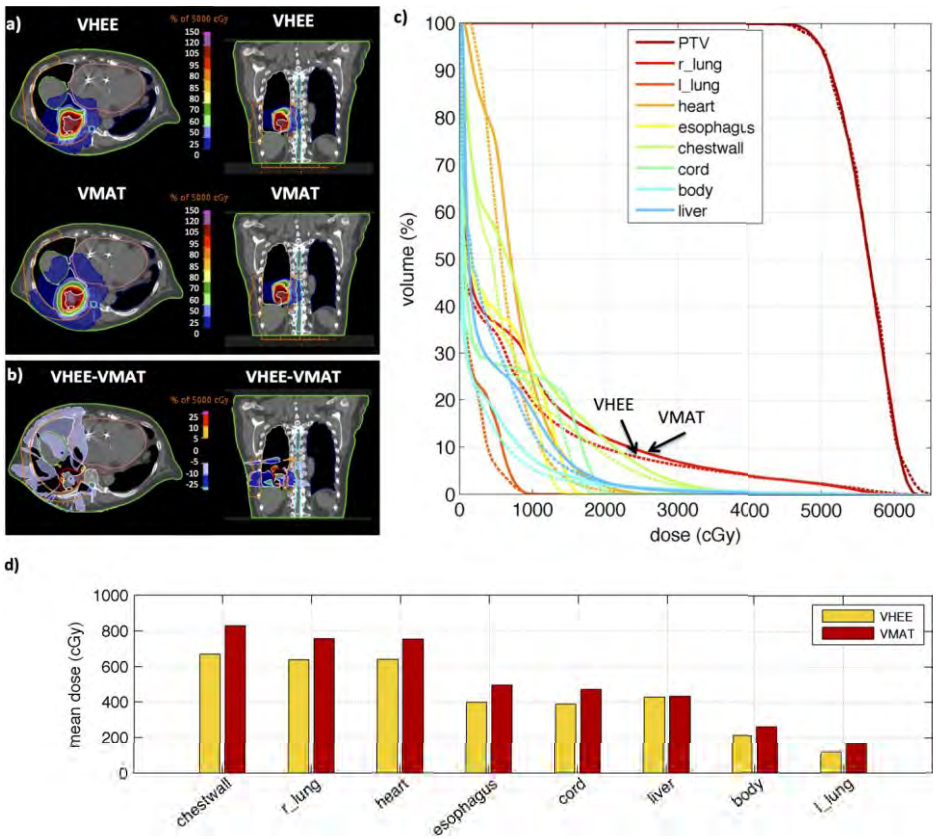

F . 7. Lung case dose distributions (a), dose difference maps (b), DVHs (c), and organ mean doses (d) for a 100 MeV VHEE plan and the clinical 6 MV FFF VMAT plan.

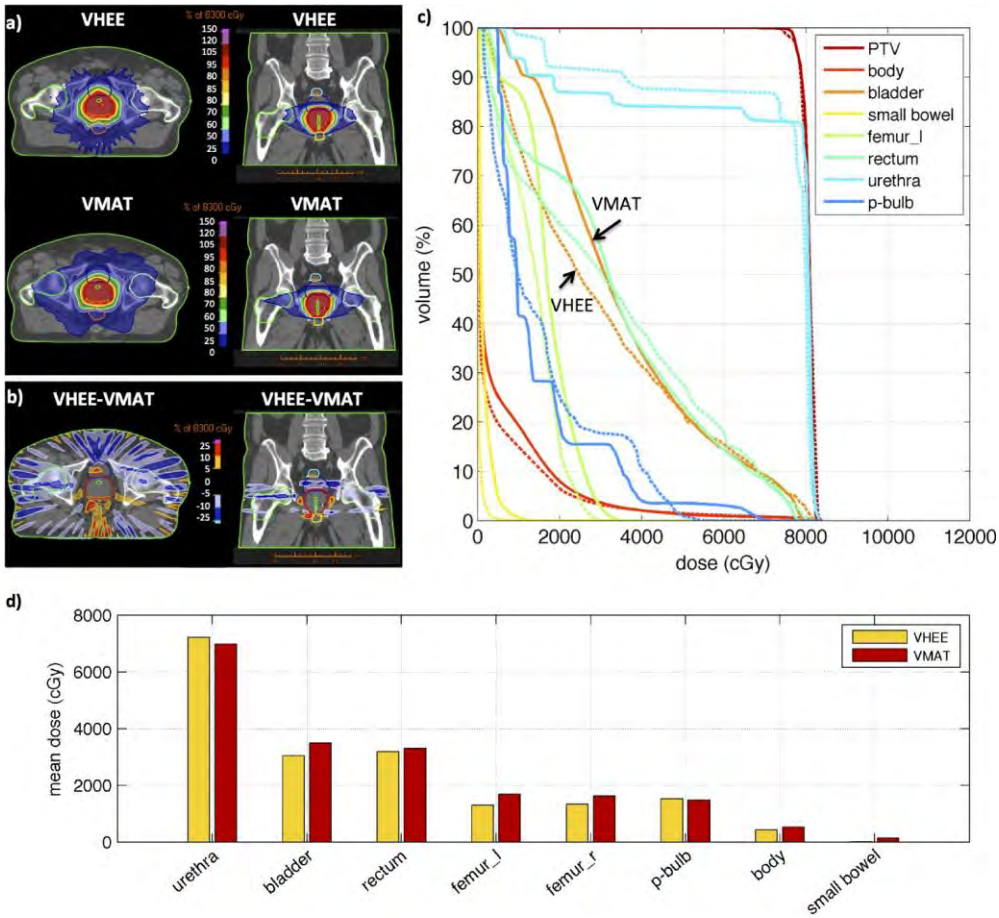

F . 8. Prostate case dose distributions (a), dose difference maps (b), DVHs (c), and organ mean doses (d) for a 100 MeV VHEE plan and the clinical 15 MV VMAT plan.

dose distribution was similar to the clinical VMAT plans. One of the advantages of VHEE radiotherapy over photon beam radiotherapy is the potentially short treatment time that we can estimate based on the parameters of existing linear accelerators if we assume they can in principle accelerate electrons to 100 MeV. We calculated that about 30 times lower number of 6–100 MeV electrons is needed to deliver the same dose at 3 cm depth compared to 15 MV photons. Under the assumption that the TrueBeam machine (Varian Medical, Palo Alto, CA) delivers dose rates of 14 Gy/min in the 6 MV FFF mode and the estimated 6% x-ray beam production efficiency in a 6 MV FFF mode,[5] the dose rate of a 100 MeV electron beam could be approximately 117 Gy/s. If VHEE pencil beam scanning time is ignored, even large VHEE treatment doses can be in principle delivered in subsecond times. Note that clinical VMAT plan delivery times are limited by the limited gantry rotation speed, which is currently 1 rotation/min, in addition to dose rate.

The EGSnrc MC codes used in this work do not simulate the generation and transport of neutrons and protons, nor do they take into account dose deposition due to activation of radionuclides in the tissue. However, recent work by Subiel *et al.* investigated the effect of these processes on dose deposition in EBT2 Gafchromic films and concluded that both contributions to film doses were negligible.[15] Since EBT2 Gafchromic films are made of tissue-equivalent materials, these film results can be applied to human tissues.

The EGSnrc MC codes were selected for VHEE dose calculations, because we validated EGSnrc VHEE dose calculations in a homogeneous phantom against experimental data acquired on a 70 MeV beam line at SLAC National Accelerator Laboratory.[11] Other MC codes, such as 4 (Ref. 16) or ,[17] could have been considered for VHEE pencil beam dose calculations. 4 has already been used for VHEE dose calculations;[18] however, its longer dose calculation times[19] compared to EGSnrc make it a less suitable code for VHEE treatment planning. could possibly be a suitable code for simulations of VHEE beams, thanks to its more accurate low energy electron and photon transport; however, it should first be compared against VHEE experimental data or other validated MC codes.

Based on the presented pediatric, lung, and prostate cases, we could conclude that a VHEE treatment machine could consist of a 100 MeV accelerator capable of delivery of 36 beams scanned in 2 mm intervals. In order to identify optimal parameters of a VHEE treatment machine suitable for treatments of a large variety of cases, treatment planning for a larger number of clinical sites including lung, pelvis, head and neck, and liver will be performed in future work. The presented treatment planning workflow with the

GUI for pencil beam MC dose calculation will serve as an invaluable tool for such a study. We will also investigate the possibility of using noncoplanar VHEE beams for treatment planning that may have further dosimetric advantages.

5. CONCLUSIONS

We have presented treatment planning for radiotherapy delivered with very high-energy electron scanning beams and we compared VHEE plans to state-of-the-art VMAT plans for three clinical cases. The presented treatment planning approach is based on patient-specific Monte Carlo dose calculations of VHEE pencil beams followed by spot scanning optimization in a research version of RayStation, a commercially available treatment planning platform. We created a GUI for facilitation of VHEE pencil beam MC calculations, in which various VHEE treatment parameters can be varied. Using the GUI, the optimal VHEE RT parameters of the ones we investigated for a pediatric case were identified to be 100 MeV 1 mm FWHM electron pencil beams scanned on a 2-mm grid and delivered from 36 angles with 40 cm SAD.

We have furthermore demonstrated the dosimetric advantage of VHEE radiotherapy over photon VMAT radiotherapy for three cases. For the pediatric case, VHEE dose to all critical organs was up to 70% lower than the clinical 6 MV VMAT dose for the same target coverage. We have shown that pediatric patients might benefit from treatments with VHEE, as the VHEE integral dose was decreased by 33% compared to the VMAT plan. We have also shown that VHEE lung case dose distribution was superior to the clinical VMAT plan and the VHEE dose distribution for prostate case was similar to the clinical VMAT plan. In summary, the presented dosimetric study indicates that VHEE radiotherapy should be further investigated as a possible cancer treatment modality. Our treatment planning workflow has the potential to become a practical tool for evaluating VHEE plans of arbitrary machine geometry.

ACKNOWLEDGMENTS

First of all, the authors would like to acknowledge the provision of software and excellent engineering support that we received from RaySearch Laboratories under a research agreement. The authors would also like to acknowledge support for this work from the Weston Havens Foundation, the Li Ka Shing Foundation, a Research Seed Grant from the American Association of Physicists in Medicine, a Stanford Bio-X Interdisciplinary Initiatives Program Award, Stanford Department of Radiation Oncology, Stanford University School of Medicine, Stanford University Office of the Provost, and a U.S. Department of Defense Lung Cancer Research Program Idea Development Award No. W81XWH-12-LCRP-IDA.

[a]Authors to whom correspondence should be addressed. Electronic addresses: Peter.Maxim@Stanford.edu; Telephone: 650-725-4099; Fax: 650-498-5008 and BWLoo@Stanford.edu; Telephone: 650-736-7143; Fax: 650-725-8231.

[1]C. DesRosiers, V. Moskvin, A. F. Bielajew, and L. Papiez, "150-250 MeV electron beams in radiation therapy," Phys. Med. Biol. **45**, 1781–1805 (2000).
[2]L. Papiez, C. DesRosiers, and V. Moskvin, "Very high energy electrons (50-250 MeV) and radiation therapy," Technol. Cancer Res. Treat. **1**, 105–110 (2002).
[3]C. Yeboah, G. A. Sandison, and V. Moskvin, "Optimization of intensity-modulated very high energy (50-250 MeV) electron therapy," Phys. Med. Biol. **47**, 1285–1301 (2002).
[4]C. Yeboah and G. A. Sandison, "Optimized treatment planning for prostate cancer comparing IMPT, VHEET and 15 MV IMXT," Phys. Med. Biol. **47**, 2247–2261 (2002).
[5]J. V. Siebers, P. J. Keall, B. Libby, and R. Mohan, "Comparison of EGS4 and MCNP4b Monte Carlo codes for generation of photon phase space distributions for a varian 2100C," Phys. Med. Biol. **44**, 3009–3026 (1999).
[6]B. W. Loo, P. G. Maxim, and V. A. Dolgashev, "Pluridirectional very high electron energy radiation therapy systems and processes," U.S. patent 8,618,521 (U.S. Patent and Trademark Office, Washington, DC, December 31, 2013).
[7]V. Dolgashev, S. Tantawi, Y. Higashi, and B. Spataro, "Geometric dependence of radio-frequency breakdown in normal conducting accelerating structures," Appl. Phys. Lett. **97**, 171501 (2010).
[8]I. Kawrakow and D. W. O. Rogers, "The EGSnrc code system: Monte Carlo simulation of electron and photon transport," Technical Report PIRS-701 (NRCC, 2006).
[9]D. W. O. Rogers, B. A. Faddegon, G. X. Ding, C. M. Ma, J. We, and T. R. Mackie, "BEAM–A Monte-Carlo code to simulate radiotherapy treatment units," Med. Phys. **22**, 503–524(1995).
[10]B. R. B. Walters, I. Kawrakow, and D. W. O. Rogers, "DOSXYZnrc users manual," NRCC Report PIRS-794revB (NRCC, 2007).
[11]M. Bazalova-Carter, M. Liu, B. Palma, M. Dunning, D. McCormick, E. Hemsing, J. Nelson, K. Jobe, E. Colby, A. C. Koong, S. Tantawi, V. Dolgashev, P. G. Maxim, and B. W. Loo, Jr., "Comparison of film measurements and Monte Carlo simulations of dose delivered with very high-energy electron beams in a polystyrene phantom," Med. Phys. **42**, 1606–1613 (2015).
[12]J. Radon, "On determination of functions by their integral values along certain multiplicities," Ber. der Sachische Akademie der Wissenschaften Leipzig (Germany) **69**, 262–277 (1917).
[13]M. J. Berger, J. H. Hubbell, S. M. Seltzer, J. Chang, J. S. Coursey, R. Sukumar, and D. Zucker, "XCOM: Photon cross section database," NBSIR 87-3597 in web version 1.3 (2005), http://physics.nist.gov/PhysRefData/Xcom/Text/XCOM.html.
[14]U. Oelfke and T. Bortfeld, "Inverse planning for photon and proton beams," Med. Dosim. **26**, 113–124 (2001).
[15]A. Subiel, V. Moskvin, G. H. Welsh, S. Cipiccia, D. Reboredo, P. Evans, M. Partridge, C. DesRosiers, M. P. Anania, A. Cianchi, A. Mostacci, E. Chiadroni, D. Di Giovenale, F. Villa, R. Pompili, M. Ferrario, M. Belleveglia, G. Di Pirro, G. Gatti, C. Vaccarezza, B. Seitz, R. C. Isaac, E. Brunetti, S. M. Wiggins, B. Ersfeld, M. R. Islam, M. S. Mendonca, A. Sorensen, M. Boyd, and D. A. Jaroszynski, "Dosimetry of very high energy electrons (VHEE) for radiotherapy applications: Using radiochromic film measurements and monte carlo simulations," Phys. Med. Biol. **59**, 5811–5829 (2014).
[16]S. Agostinelli, J. Allison, K. Amako, J. Apostolakis, H. Araujo, P. Arce, M. Asai, D. Axen, S. Banerjee, G. Barrand, F. Behner, L. Bellagamba, J. Boudreau, L. Broglia, A. Brunengo, H. Burkhardt, S. Chauvie, J. Chuma, R. Chytracek, G. Cooperman, G. Cosmo, P. Degtyarenko, A. Dell'Acqua, G. Depaola, D. Dietrich, R. Enami, A. Feliciello, C. Ferguson, H. Fesefeldt, G. Folger, F. Foppiano, A. Forti, S. Garelli, S. Giani, R. Giannitrapani, D. Gibin, J. J. G. Cadenas, I. Gonzalez, G. G. Abril, G. Greeniaus, W. Greiner, V. Grichine, A. Grossheim, S. Guatelli, P. Gumplinger, R. Hamatsu, K. Hashimoto, H. Hasui, A. Heikkinen, A. Howard, V. Ivanchenko, A. Johnson, F. W. Jones, J. Kallenbach, N. Kanaya, M. Kawabata, Y. Kawabata, M. Kawaguti, S. Kelner, P. Kent, A. Kimura, T. Kodama, R. Kokoulin, M. Kossov, H. Kurashige, E. Lamanna, T. Lampen, V. Lara, V. Lefebure, F. Lei, M. Liendl, W. Lockman, F. Longo, S. Magni, M. Maire, E. Medernach, K. Minamimoto, P. M. de Freitas, Y. Morita, K. Murakami, M. Nagamatu, R. Nartallo, P. Nieminen, T. Nishimura, K. Ohtsubo, M. Okamura, S. O'Neale, Y. Oohata, K. Paech, J. Perl, A. Pfeiffer, M. G. Pia, F. Ranjard, A. Rybin, S. Sadilov, E. Di Salvo, G. Santin, T. Sasaki, N. Savvas, Y. Sawada, S.

Scherer, S. Seil, V. Sirotenko, D. Smith, N. Starkov, H. Stoecker, J. Sulkimo, M. Takahata, S. Tanaka, E. Tcherniaev, E. S. Tehrani, M. Tropeano, P. Truscott, H. Uno, L. Urban, P. Urban, M. Verderi, A. Walkden, W. Wander, H. Weber, J. P. Wellisch, T. Wenaus, D. C. Williams, D. Wright, T. Yamada, H. Yoshida, and D. Zschiesche, "4-a simulation toolkit," Nucl. Instrum. Methods Phys. Res., Sect. A **506**, 250–303 (2003).

[17]J. Baro, J. Sempau, J. M. Fernandezvarea, and F. Salvat, "PENELOPE–An algorithm for Monte-Carlo simulation of the penetration and energy-loss of electrons and positrons in matter," Nucl. Instrum. Methods Phys. Res., Sect. B **100**, 31–46 (1995).

[18]O. Lundh, C. Rechatin, J. Faure, A. Ben-Ismaïl, J. Lim, C. De Wagter, W. De Neve, and V. Malka, "Comparison of measured with calculated dose distribution from a 120-MeV electron beam from a laser-plasma accelerator," Med. Phys. **39**, 3501–3508 (2012).

[19]I. J. Chetty, B. Curran, J. E. Cygler, J. J. DeMarco, G. Ezzell, B. A. Faddegon, I. Kawrakow, P. J. Keall, H. Liu, C. M. C. Ma, D. W. O. Rogers, J. Seuntjens, D. Sheikh-Bagheri, and J. V. Siebers, "Report of the AAPM Task Group No. 105: Issues associated with clinical implementation of Monte Carlo-based photon and electron external beam treatment planning," Med. Phys. **34**, 4818–4853 (2007).

Elsevier Editorial System(tm) for Radiotherapy and Oncology
Manuscript Draft

Manuscript Number:

Title: Assessment of the quality of very high-energy electron radiotherapy treatment planning: Five clinical cases.

Article Type: Full Length Article

Keywords: Very high-energy electrons; Monte Carlo; treatment planning; integral dose.

Corresponding Author: Dr. Bianey Atriana Palma, Ph.D.

Corresponding Author's Institution: Stanford University

First Author: Bianey Atriana Palma, Ph.D.

Order of Authors: Bianey Atriana Palma, Ph.D.; Magdalena Bazalova-Carter, Ph.D.; Björn Hårdemark, Ph.D.; Elin Hynning, Ph.D.; Bradley Qu; Billy W Loo, M.D. Ph.D.; Peter G Maxim, Ph.D.

Abstract: Purpose: To assess the quality of very-high energy electron (VHEE) scanning pencil beam radiation therapy in relation to state-of-the-art volumetric modulated arc therapy (VMAT) and to determine the extent of its application.
Materials/Methods: We planned five clinical cases with VHEE scanning pencil beams of 100 and 120 MeV, equally distributed in a coplanar arrangement around the patient. The clinical cases included acoustic neuroma, and liver, lung, esophagus, and anal cancer cases. We performed Monte Carlo (MC) dose calculations and we optimized the dose in a research version of RayStation. VHEE plan performance was compared against clinically delivered VMAT.
Results: With equal target coverage, mean doses to organs at risk (OARs) were on average 22% lower for the VHEE plans compared to the VMAT plans. Dose conformity was equal or superior compared to the VMAT plans and integral dose to the body was in average 14% (9%-22%) lower for theVHEE plans.
Conclusions: The dosimetric advantages of VHEE as demonstrated for a variety of clinical cases, combined with the theoretical ultra fast treatment delivery, afford VHEE scanning pencil beam radiotherapy a suitable and potentially superior alternative for cancer radiotherapy.

Cover Letter

STANFORD
UNIVERSITY
MEDICAL CENTER
Hospital & Clinics · School of Medicine

DEPARTMENT OF RADIATION ONCOLOGY
http://radonc.stanford.edu

Quynh-Thu Le, M.D., F.A.C.R.
Katharine Dexter McCormick & Stanley McCormick Memorial Professor & Chair

Amato J. Giaccia, Ph.D.
Jack, Lulu & Sam Willson Professor in Cancer Biology
Division Director & Associate Chair for Research

Albert C. Koong, M.D., Ph.D.
Associate Professor & Associate Chair for Clinical Operations

Stanford Cancer Center
875 Blake Wilbur Drive
Stanford, CA 94305-5847
T: 650.723.6171
F: 650.725.8231

Division of Radiation Therapy

Sarah S. Donaldson, M.D., F.A.C.R.
Catharine & Howard Avery Professor

Richard T. Hoppe, M.D., F.A.C.R.
Henry S. Kaplan-Harry Lebeson Professor of Cancer Biology

Daniel T. Chang, M.D.
Maximilian Diehn, M.D., Ph.D.
Iris C. Gibbs, M.D.
Steven L. Hancock, M.D., F.A.C.R.
Wendy Hara, M.D.
Kathleen C. Horst, M.D.
Elizabeth A. Kidd, M.D.
Susan J. Knox, Ph.D., M.D.
Billy W. Loo, M.D., Ph.D.
Lynn Million, M.D.
Scott G. Soltys, M.D.

Don R. Goffinet, M.D.
Emeritus

Daniel S. Kapp, M.D., Ph.D.
Emeritus

Division of Radiation Physics

Lei Xing, Ph.D.
Jacob Haimson Professor in Radiation Physics & Division Director

Sonja Dieterich, Ph.D., D.A.B.R.
Edward E. Graves, Ph.D.
Dimitre Hristov, Ph.D.
Gary Luxton, Ph.D.
Peter G. Maxim, Ph.D.

Peter Fessenden, Ph.D.
Emeritus

Division of Radiation & Cancer Biology

CCSR-South, Room 1255
269 Campus Drive
Stanford, CA 94305-5152

Laura D. Attardi, Ph.D.
J. Martin Brown, D. Phil
Nicholas C. Denko, M.D., Ph.D.

July 27, 2015

Professor Jens Overgaard, M.D.
Editor-in-Chief, *Radiotherapy and Oncology*

Dear Dr. Overgaard:

We would like to submit our manuscript entitled "Assessment of the quality of very high-energy electron radiotherapy treatment planning: Five clinical cases." for consideration for publication in *Radiotherapy and Oncology*. The use of very high-energy electron (VHEE) beams of 100-120 MeV has attractive properties for radiation therapy including the promise of reducing the irradiation time. In this work we investigated the advantages and limitations of VHEE radiotherapy compared to the state-of-the-art VMAT-plans in five representative anatomical sites using Monte Carlo dose calculations. The objective was to determine the cases that may benefit the most and the combination of beam parameters that could lead to a successful treatment planning and finally to the design of our VHEE treatment machine.

All of the work reported is original and was performed at Stanford University. All procedures were in accordance with the ethical standards established by the Stanford Institutional Review Board. No human or animal subjects were involved in this study. This work has not been previously published and is not under consideration for publication elsewhere. All authors qualified for authorship. Submitted electronically along with the cover letter are the original manuscript, figures, and tables according to the instructions for online submission.

Bianey Palma, Bradley Qu and Magdalena Bazalova-Carter declare no conflicts of interest. Björn Hårdemark and Elin Hynning work for RaySearch Laboratories. Dr. Loo, and I have each received research funding from Varian Medical Systems. Dr. Loo and I have also received speaking honoraria from Varian Medical Systems and we also received research support from RaySearch Laboratories. Dr. Loo has also received research support from General Electric and Philips.

Otherwise, we have no financial or other relationships, which may lead to a conflict of interest.
Please note that there are two corresponding authors, Billy W Loo and Peter G. Maxim.

If you have any questions, please do not hesitate to contact me at (+1) 650-724-3018 or pmaxim@stanford.edu. Thank you very much for your consideration.

Sincerely,

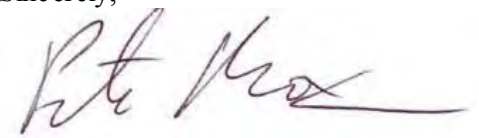

Peter G. Maxim, Ph.D.
Assistant Professor
Department of Radiation Oncology and Stanford Cancer Institute
Stanford University School of Medicine

TITLE: Assessment of the quality of very high-energy electron radiotherapy treatment planning: Five clinical cases.

AUTHORS: Bianey Palma[1], Magdalena Bazalova-Carter[1], Björn Hårdemark[2], Elin Hynning[2], Bradley Qu[1], Billy W. Loo, Jr.[1], and Peter G. Maxim[1].
(1) Department of Radiation Oncology, Stanford University, Stanford, CA 94305, USA
(2) RaySearch Laboratories AB, Stockholm, Sweden

***CO-CORRESPONDING AUTHORS**

Billy W. Loo Jr., M.D. Ph.D.
Department of Radiation Oncology and Stanford Cancer Institute
Stanford University School of Medicine
875 Blake Wilbur Drive
Stanford, CA 94305-5847
E-mail: BWLoo@Stanford.edu
Tel: 650-736-7143; Fax: 650-725-8231

AND

Peter G. Maxim, Ph.D.
Department of Radiation Oncology and Stanford Cancer Institute
Stanford University School of Medicine
875 Blake Wilbur Drive
Stanford, CA 94305-5847
E-mail: Peter.Maxim@Stanford.edu
Tel: 650-725-4099; Fax: 650-498-5008

Number of tables: 1
Number of figures: 5
Running head (shortened form of title): VHEE radiotherapy treatment planning

Keywords: Very high-energy electrons, Monte Carlo, treatment planning, integral dose

Abstract

Purpose: To assess the quality of very-high energy electron (VHEE) scanning pencil beam radiation therapy in relation to state-of-the-art volumetric modulated arc therapy (VMAT) and to determine the extent of its application.

Materials/Methods: We planned five clinical cases with VHEE scanning pencil beams of 100 and 120 MeV, equally distributed in a coplanar arrangement around the patient. The clinical cases included acoustic neuroma, and liver, lung, esophagus, and anal cancer cases. We performed Monte Carlo (MC) dose calculations and we optimized the dose in a research version of RayStation. VHEE plan performance was compared against clinically delivered VMAT.

Results: With equal target coverage, mean doses to organs at risk (OARs) were on average 22% lower for the VHEE plans compared to the VMAT plans. Dose conformity was equal or superior compared to the VMAT plans and integral dose to the body was in average 14% (9%-22%) lower for the VHEE plans.

Conclusions: The dosimetric advantages of VHEE as demonstrated for a variety of clinical cases, combined with the theoretical ultra fast treatment delivery, afford VHEE scanning pencil beam radiotherapy a suitable and potentially superior alternative for cancer radiotherapy.

1. Introduction

The use of electron beams in radiation therapy has been limited to the treatment of superficial lesions due to electrons short range at the clinically available energies. Previous studies have shown the potential advantages of using very high energy electrons (VHEE) of 100 MeV to 250 MeV for the treatment of deep-seated lesions [1-4]. VHEE beams are characterized by a penetrating ability comparable to clinical photon beams in tissue (>40 cm for 150 MeV [1]), reduced scattering in air and tissue, and absence of electronic disequilibrium at interfaces with varying densities which favors a more uniform dose distribution throughout the target [1, 2]. These VHEE physical characteristics contribute to enhance the ratio of target dose to dose to healthy tissue [4, 5]. Additionally, VHEE radiation therapy could be delivered using pencil beam electromagnetic scanning techniques, eliminating with this the dependence on moving mechanical devices, opening the possibility of a very fast irradiation.

These ideas led our group to propose a conceptual design of a compact treatment machine able to deliver VHEE scanning pencil beams from multiple angles using fixed beam lines equally-spaced in a coplanar arrangement around the patient [6]. Pencil beams of adjustable sizes, would be rapidly raster-scanned over an area covering the beam's-eye-view of the target to produce intensity-modulated fields from each beam's direction. A high-efficiency and high-gradient LINAC design [7] would be required for the system to fit in existing radiation therapy vaults. Before facing the technical challenges of building a VHEE machine it would be necessary to determine: 1) the cases that may be treated with VHEE radiation therapy and 2) the combination of beam parameters that could lead to a successful treatment planning and that would become the input for the design of our VHEE treatment machine.

In a previous work [5] we presented the workflow for radiotherapy with very high-energy electron beams and demonstrated the superiority of VHEE dose distribution for a pediatric brain case and a lung case as well as its equivalence for a prostate case compared to volumetric modulated arc therapy (VMAT). The present study aimed to extend the application of VHEE treatment planning to a larger number of anatomic sites considering a realistic pencil beam emittance [8]. In this work we presented VHEE dose distributions for five clinical cases calculated by means of Monte Carlo simulations. We also included a comparison between VHEE and the clinically delivered VMAT dose distributions to state the quality of VHEE plans compared to the current state-of-the-art photon radiation therapy technique.

2. Materials and methods

We selected five clinical cases to be planned for radiotherapy with VHEE pencil beam scanning. VHEE pencil beams of energies 100 and 120 MeV and sizes of 0.1-0.5 cm full width at half maximum (FWHM) were calculated using BEAMnrc/EGSnrc [9, 10] MC code. Phase space data (PSD) was generated considering a monoenergetic elliptical beam with Gaussian distribution and an emittance of 0.3° (half-angle). The beam emittance was set based on the characteristics of the high energy electron beam from the Next Linear Collider Test Accelerator (NLCTA) located at the SLAC National Accelerator Laboratory [8].

We considered an array of multiple fixed coplanar beam lines (16 or 32) equally spaced around the patient with a 50 cm distance from the end of the electron beam line to the isocenter. The spacing between pencil beams could also be modified (from 0.1 cm to 0.5 cm at isocenter).

2.1 VHEE treatment planning

We ran DOSxyz /EGSnrc [12] MC simulations for pencil beam dose calculation using a Matlab (The Mathworks, Nattick, MA) graphical user interface (GUI) developed by our group [5] and we optimized the resultant dose distributions in RayStation (RaySearch Laboratories AB, Stockholm Sweden).

2.1.2 VHEE pencil beam dose optimization

The objectives and constraints for the VHEE pencil beam dose spot-scanning optimization were set based on the dose volume histogram (DVH) of the corresponding VMAT plan. VHEE and VMAT plans were normalized so 95% of the PTV was covered by 100% of the prescription dose, which is how the clinically delivered VMAT plans were prescribed.

We calculated DVHs, mean dose to the organs at risk (OARs) and conformity indices CI_{100} and CI_{50}. Conformity index CI_x was defined as the ratio between the volume covered by x% of the prescription dose and the planning target volume (PTV).

2.2 Clinical cases

The studied clinical cases were: acoustic neuroma, and liver, lung, esophagus and anal cancer cases. Target sizes ranged from 1.2 cm^3 to 990.4 cm^3 (Table 1).

Four of the cases were treated using coplanar VMAT. Only the acoustic neuroma case was treated with non-coplanar 6MV photon beams from a CyberKnife (CK) robotic stereotactic radiosurgery system (Accuray, Sunnyvale, CA) [12].

Several VHEE plans, with different energy (100 and 120MeV), pencil beam size/spacing (0.1-0.5 cm/0.1-0.5 cm) and number of equidistant coplanar beams (16 or 32) were generated for each clinical case. We then compared the VHEE plans with each other and selected the one that provided the highest dose sparing to OARs and the highest dose conformity to compare it with the clinically delivered VMAT plan. In this work we present only the best VHEE plan for each clinical case.

3. Results

3.1 Clinical cases

3.1.1. Anal cancer case

The anal case had two PTV structures with prescription doses of 40 Gy and 45 Gy. A comparison between the dose distributions of the VHEE plan and the 15 MV VMAT plan (3 arcs) is shown in Figure 1.

VHEE plan consisted of 32 100 MeV beams and a pencil beam size/spacing of 0.5 cm/0.5 cm. The VHEE plan provided the same target coverage as the VMAT plan to both PTV structures. Furthermore, the VHEE plan was more conformal than the VMAT plan in all selected planes: axial, coronal and sagittal (Figure 1-a). This was confirmed by indices CI_{100} and CI_{50}. The

144 CI_{50}=4.94 of the VHEE plan was lower than the CI_{50}=6.69 of VMAT. CI_{100} indices were similar for the two plans (Table 1).

The DVH comparison (Figure 1-b) demonstrated the superior normal tissue dose sparing provided by the VHEE plan. In general, the VHEE plan reduced the mean doses to most of the
148 OARs (Figure 1-c), including a reduction of 21.8% and 18.5% to the genitalia and perineum, respectively. Also, the integral dose (mean dose to the body structure) was reduced by 13% when planning with VHEE pencil beams.

152 3.1.2. Esophagus cancer case

This case also had two PTV structures, with prescription doses of 45 Gy and 50 Gy. Figure 2 shows the comparison between the 6MV VMAT plan (3 arcs) and the corresponding VHEE plan.
156 The VHEE plan was composed of 32 120 MeV beams with pencil beam size/spacing of 0.5 cm/0.5 cm.

The VHEE plan was more conformal than the VMAT plan for the two PTV structures as can be seen from the dose distributions in Figure 2-a. Conformity indices CI_{100}=1.05 and CI_{50}=3.18 of
160 the VHEE plan were lower than the CI_{100}=1.09 and CI_{50}=4.78 of the VMAT plan. DVHs showed a general OARs dose reduction when using VHEE (Figure 2-b) especially for doses lower than 35 Gy (~76% of the prescription dose). OARs mean doses were systematically lower for the VHEE plan (Figure 2-c) with a 23.2% and 19.6% lower mean dose to the spinal cord and heart,
164 respectively. The integral dose was also reduced by a 22% when using VHEE pencil beams.

3.1.3. Lung cancer case

The comparison between the 10 MV VMAT plan (1 arc) and the corresponding VHEE plan showed the same PTV coverage and dose homogeneity for both plans (Figure 3). The VHEE plan consisted of 16 100 MeV beams. The pencil beam size/spacing was reduced accordingly to the target size (Table 1) to 0.3 cm/0.3 cm.

The difference between the plan's DVHs was more subtle than for the previous clinical cases. However, the mean doses for all the OARs were still lower for the VHEE plan (Figure 3-c) with the bronchial tree receiving 20.9% lower dose. Integral dose in this case was reduced by a 9.6% when using VHEE pencil beams. This modest reduction in integral dose was also reflected in the 12.9% difference between the conformity indices CI_{50}= 2.98 for the VHEE plan and 3.42 for the VMAT plan. CI_{100}=0.95 of the VHEE was lower than the CI_{100}=0.97 of the VMAT, fulfilling accurately the prescription dose.

3.1.4. Liver cancer case

The target volume in this case was smaller (9.3 cm^3) and more superficial ~ 6 cm in depth (Figure 4-a). The VHEE plan consisted of 32 120 MeV beams and pencil beam size/spacing of 0.3 cm/0.3 cm. A comparison between the VHEE plan and the 10 MV VMAT plan (1 arc) is presented in Figure 4. The VHEE plan was more heterogeneous than the VMAT plan, as shown by the DVH comparison in Figure 4-b. Maximum dose to the PTV, defined as the dose to 2% of the volume, was 115.0% and 127.3% of the prescribed dose for the VMAT and VHEE plans, respectively. However, in this case, due to the reduced size of the PTV, a higher dose > 120% of the prescription dose to the target volume was desirable, and as shown by the dose distributions and DVH, achievable when using VHEE pencil beams. The PTV dose increase was not

accompanied by a scale in dose to the OARs. As shown in Figure 4-c, OARs mean doses were very similar between the plans. The most relevant difference between the plans was an 18.7% lower dose to the chest wall for the VHEE plan. Conformity indices CI_{100} (0.99 for VMAT and 0.98 for VHEE) and CI_{50} (4.36 for VMAT and 3.25 for VHEE) showed the higher conformity of the VHEE plan. However, integral dose was not significantly different between the plans.

3.1.5. Acoustic neuroma case

The PTV in this case had a volume of only 1.2 cm^3 and was located at a maximum depth of 11.6 cm in the AP direction. The VHEE plan was composed of 32 120 MeV beams and pencil beam size/spacing of 0.1 cm/0.1 cm. A comparison between the VHEE treatment plan and the clinically delivered CyberKnife plan (84 beams) is presented in Figure 5.

In order to make a fair comparison amongst coplanar plans, an additional 6 MV VMAT plan (2 arcs) was calculated. The comparison between dose distributions (Figure 5-a) showed the high conformity of the CK plan, followed by the VHEE and the VMAT plan, in that order, as confirmed by their conformity indices. CI_{100}=1.22 and CI_{50}=8.91 of VHEE treatment plan were higher than the CI_{100}=1.06 and CI_{50}=5.59 of the CK plan but lower than the CI_{100}=1.36 and CI_{50}=9.23 of the VMAT plan. The same PTV coverage was achieved by the three plans (Figure 5-b). The most relevant difference between the plans regarding OARs dose sparing was for the right cochlea. The VHEE plan provided 12.2% lower mean dose to the right cochlea than CK but 15.4% higher mean dose than the VMAT plan. Integral dose was not significantly different between the plans.

A summary of the conformity indices CI_{100} and CI_{50} for all the cases and treatment plans is listed in Table 1.

4. Discussion

In a previous work we demonstrated that 100 MeV VHEE dose distributions for a pediatric brain case and a lung case outperformed the VMAT plans while a 100 MeV prostate dose distribution was similar to the clinical VMAT plan [5]. This work investigated the application of VHEE pencil beams to five additional anatomical sites considering a realistic pencil beam emittance of 0.3º. In order to assess the quality of VHEE treatment planning and determine the extent of its application we compared the VHEE plans to the corresponding clinically delivered VMAT plans. In all the cases, VHEE provided more conformal dose distributions and target coverage of comparable quality than that offered by VMAT. This is a consequence of the penetrating ability of very high energy electrons (>40 cm for 150 MeV) and the use of multiple equidistant beams around the patient, which maximizes the dose to the target while reducing the dose to normal tissues. The cases that benefited most of these characteristics were the ones with targets > 4 cm that were more centrally located like the anal, esophagus, and lung cases presented in this work, in agreement with literature [1]. We demonstrated that VHEE dose distributions provide a higher normal tissue dose sparing than the corresponding VMAT plan. While in the cases with smaller sized, shallower targets (acoustic neuroma and liver cancer) the VHEE dose distributions provided a similar normal tissue sparing than the VMAT plan and a more heterogeneous dose distribution inside the PTV (higher dose), which can be desirable in the case of small targets.

Based on the evaluated cases, from this and the previously published work [5], the possible parameters for the design of the VHEE treatment machine could be: 32 beams equally spaced around the patient of 100 MeV pencil beams and a scanning resolution of 0.3 cm (pencil beam size/spacing).

The lower organs mean doses and lower integral dose provided by the VHEE plans compared to the clinically delivered VMAT plans, together with the possibility of a very fast treatment delivery (of the order of ~117Gy/s [5]) support the idea of using VHEE scanning pencil beams as an alternative radiation therapy technique.

5. Conclusions

In this work we demonstrated that the use of 100 to 120 MeV very high-energy electron scanning beams for radiation therapy can be extended to other anatomic sites such as anal, esophagus, lung and liver cancer and acoustic neuroma.

We observed that, similar or superior dose distribution can be achieved by VHEE scanning pencil beam radiation therapy compared to the VMAT, even when a more realistic pencil beam emittance is considered. We confirmed that these advantages are consistent for a wide range of target volumes with an enhanced normal tissue sparing when the targets are more centrally located inside the patient (depths > 10 cm). These results, together with our previously published work [5], encouraged the design of a VHEE treatment machine [6]. The design of the VHEE treatment machine is still under investigation. In the future a design of non-coplanar VHEE beams distributed around the patient will be explored in an attempt to further improve VHEE dose distributions. In conclusion, VHEE scanning beam radiation therapy, due to its dosimetric

advantages and fast treatment delivery, has the potential to become an alternative cancer treatment modality worth of being further investigated.

Acknowledgments

The authors would like to acknowledge RaySearch Laboratories for providing the software and the technical support that we received under a research agreement. The authors would also like to acknowledge support for this work from the Weston Havens Foundation, the Li Ka Shing Foundation, a Research Seed Grant from the American Association of Physicists in Medicine, a Stanford Bio-X Interdisciplinary Initiatives Program Award, Stanford Department of Radiation Oncology, Stanford University School of Medicine, Stanford University Office of the Provost, and a U.S. Department of Defense Lung Cancer Research Program Idea Development Award No. W81XWH-12-LCRPIDA.

References

1. DesRosiers C., Moskvin V., Bielajew A.F., and Papiez L. 150-250 MeV electron beams in radiation therapy. Phys Med Biol 2000; **45**(7): 1781-805.
2. Papiez L., DesRosiers C., and Moskvin V. Very high energy electrons (50-250 MeV) and radiation therapy. Technol Cancer Res Treat 2002; **1**(2): 105-10.
3. Yeboah C., Sandison G.A., and Moskvin V. Optimization of intensity-modulated very high energy (50-250 MeV) electron therapy. Phys Med Biol 2002; **47**(8): 1285-301.
4. Yeboah C. and Sandison G.A. Optimized treatment planning for prostate cancer comparing IMPT, VHEET and 15 MV IMXT. Phys Med Biol 2002; **47**(13): 2247-61.
5. Bazalova-Carter M., Qu B., Palma B., et al., Treatment planning workflow for radiotherapy with very high-energy electron (VHEE) beams. Med Phys 2015; **42**(5): 2615-2625.
6. Loo B.W., Maxim P.G., and Dolgashev V.A. Pluridirectional very high electron energy radiation therapy systems and processes. U.S. patent, 2013. 8,618,521 (U.S. Patent and Trademark Office, Washington, DC, December, 31, 2013).
7. Dolgashev, V., Tantawi S., Higashi Y., and Spataro B. Geometric dependence of radio-frequency breakdown in normal conducting accelerating structures. Applied Physics Letters 2010; **97**(17).
8. Bazalova-Carter M., Liu M., Palma B., et al. Comparison of film measurements and Monte Carlo simulations of dose delivered with very high-energy electron beams in a polystyrene phantom. Med Phys 2015; **42**(4): 1606-1613.
9. Rogers D.W.O. The EGSnrc code system: Monte Carlo simulation of electron and photon transport. NRCC 2006.
10. Rogers D.W.O., Faddegon B.A., Ding G.X., Ma C.M., We J. and Mackie T.R. Beam: a Monte-Carlo Code to Simulate Radiotherapy Treatment Units. Med Phys 1995; **22**(5): 503-524.
11. Walters B.R.B., Kawrakow I., and Rogers D.W.O. DOSXYZnrc users manual. NRCC 2007.
12. CyberKnife Treatment Delivery. Available from: http://www.accuray.com/solutions/treatment-delivery/cyberknife-treatment-delivery.

Table 1. PTV volumes, prescription doses, and conformity indices CI_{100} and CI_{50} corresponding to the VHEE, VMAT and CK plans, for each of the studied clinical cases.

Clinical case	PTV (cm^3)	PD (Gy)	CI_{100}			CI_{50}		
			VHEE	VMAT	CK	VHEE	VMAT	CK
Anal	937.7	40	1.00	0.99	-	4.94	6.69	-
	990.4	45						
Esophagus	801.5	40	1.05	1.09	-	3.18	4.78	-
	337.9	50						
Lung	98.8	54	0.95	0.97	-	2.98	3.42	-
Liver	9.3	54	0.98	0.99	-	3.52	4.36	-
Acoustic	1.2	18	1.22	1.36	1.06	8.91	9.23	5.59

* PD: Prescription dose

Figure Legends

316

Figure 1. Anal case dose distributions (a), DVHs (VHEE in solid line and VMAT in dashed line) (b), and organ mean doses (c) for the VHEE plan and the clinically delivered 15MV VMAT plan.

Figure 2. Esophagus case dose distributions (a), DVHs (VHEE in solid line and VMAT in 320 dashed line) (b) and organ mean doses (c) for the VHEE plan and the clinically delivered 6MV VMAT plan.

Figure 3. Lung case dose distributions (a), DVHs (VHEE in solid line and VMAT in dashed line)(b), and organ mean doses (c) for the VHEE plan and the clinically delivered 10MV VMAT 324 plan.

Figure 4. Liver case dose distributions (a), DVHs (VHEE in solid line and VMAT in dashed line) (b), and organ mean doses (c) for the VHEE plan and the clinically delivered 10MV VMAT plan.

328 **Figure 5.** Acoustic case dose distributions (a), DVHs (b) and organ mean doses (c) for VHEE, 6MV VMAT and the clinically delivered CK plan.

Figure1

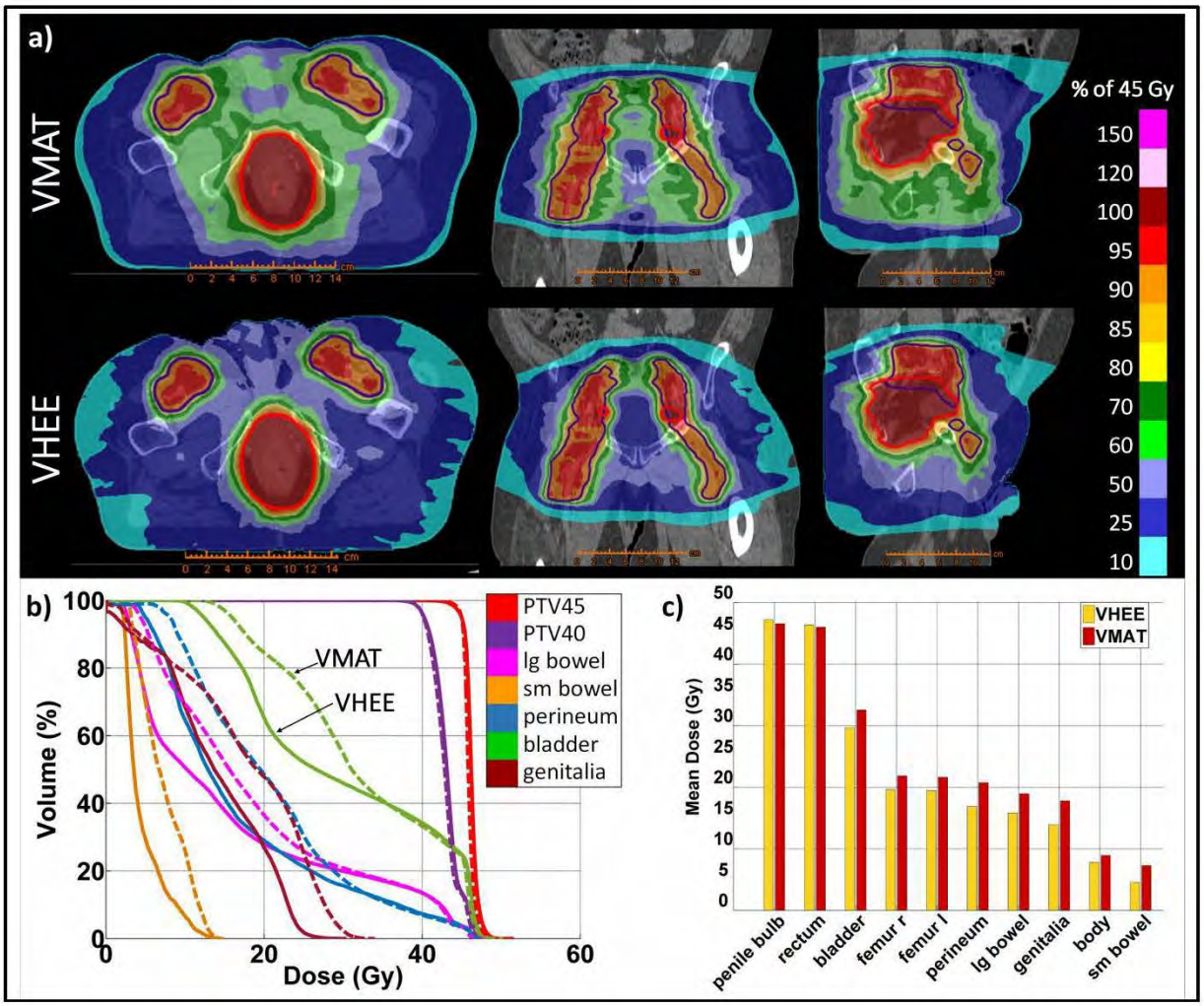
a)
VMAT
VHEE
% of 45 Gy
150
120
100
95
90
85
80
70
60
50
25
10
b)
Volume (%)
Dose (Gy)
VMAT
VHEE
PTV45
PTV40
lg bowel
sm bowel
perineum
bladder
genitalia
c)
Mean Dose (Gy)
VHEE
VMAT
penile bulb
rectum
bladder
femur r
femur l
perineum
lg bowel
genitalia
body
sm bowel

332

Figure 2

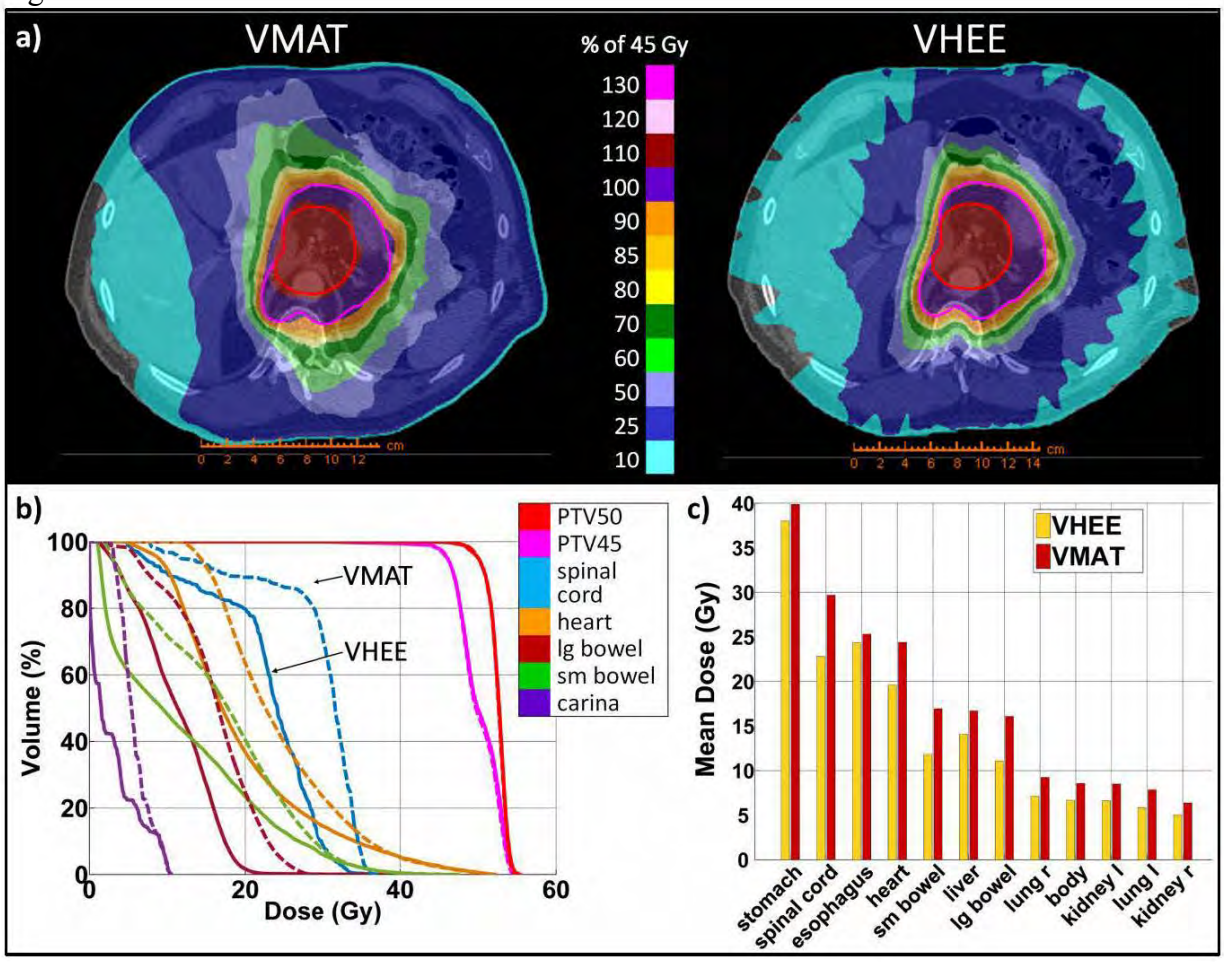
a)
VMAT
% of 45 Gy
130
120
110
100
90
85
80
70
60
50
25
10
VHEE
cm
0 2 4 6 8 10 12
0 2 4 6 8 10 12 14
b)
Volume (%)
Dose (Gy)
VMAT
VHEE
PTV50
PTV45
spinal cord
heart
lg bowel
sm bowel
carina
c)
Mean Dose (Gy)
VHEE
VMAT
stomach
spinal cord
esophagus
heart
sm bowel
liver
lg bowel
lung r
body
kidney l
lung l
kidney r

336 Figure 3

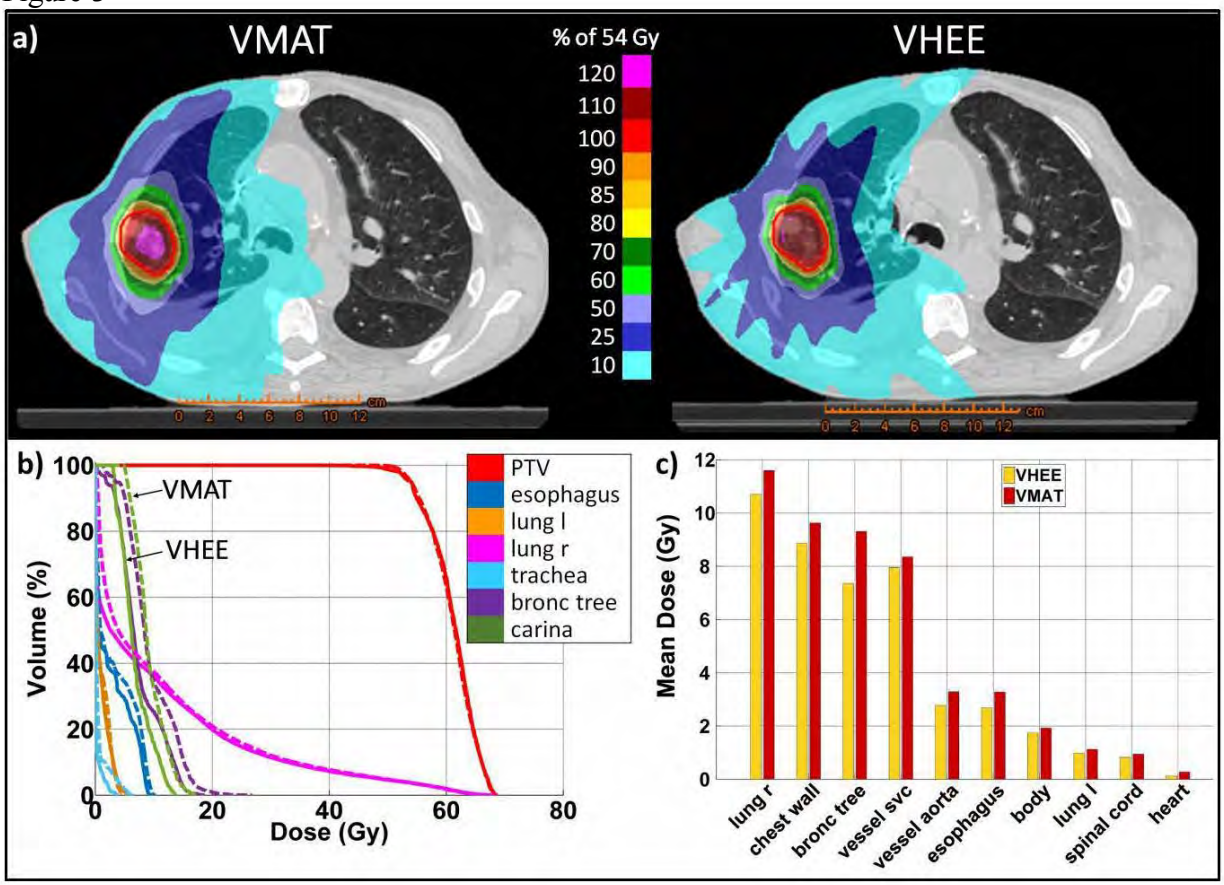
a)
VMAT
% of 54 Gy
120
110
100
90
85
80
70
60
50
25
10
VHEE
cm
0 2 4 6 8 10 12
b)
VMAT
VHEE
PTV
esophagus
lung l
lung r
trachea
bronc tree
carina
Volume (%)
Dose (Gy)
c)
VHEE
VMAT
Mean Dose (Gy)
lung r
chest wall
bronc tree
vessel svc
vessel aorta
esophagus
body
lung l
spinal cord
heart

Figure 4

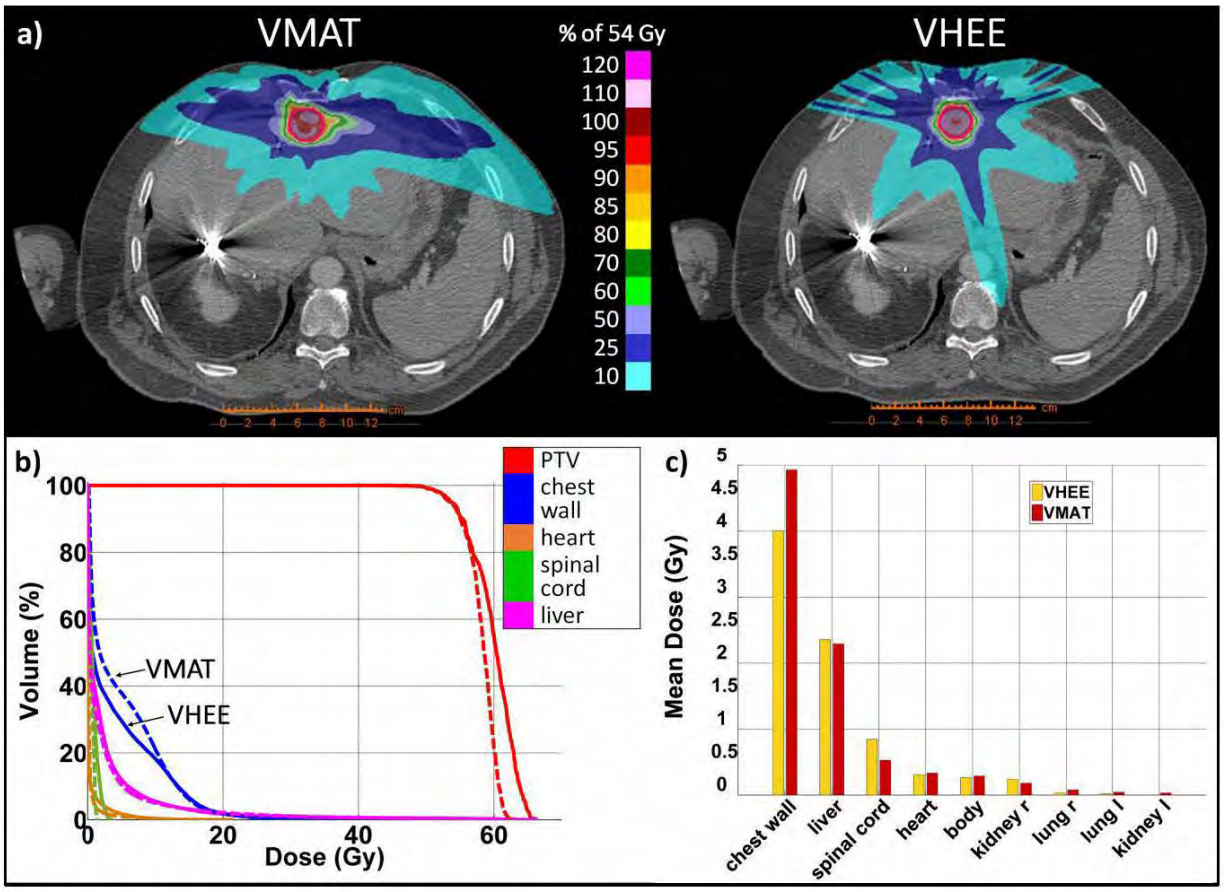
a)
VMAT
% of 54 Gy
120
110
100
95
90
85
80
70
60
50
25
10
VHEE
b)
Volume (%)
Dose (Gy)
PTV
chest wall
heart
spinal cord
liver
VMAT
VHEE
c)
Mean Dose (Gy)
VHEE
VMAT
chest wall
liver
spinal cord
heart
body
kidney r
lung r
lung l
kidney l

Figure 5

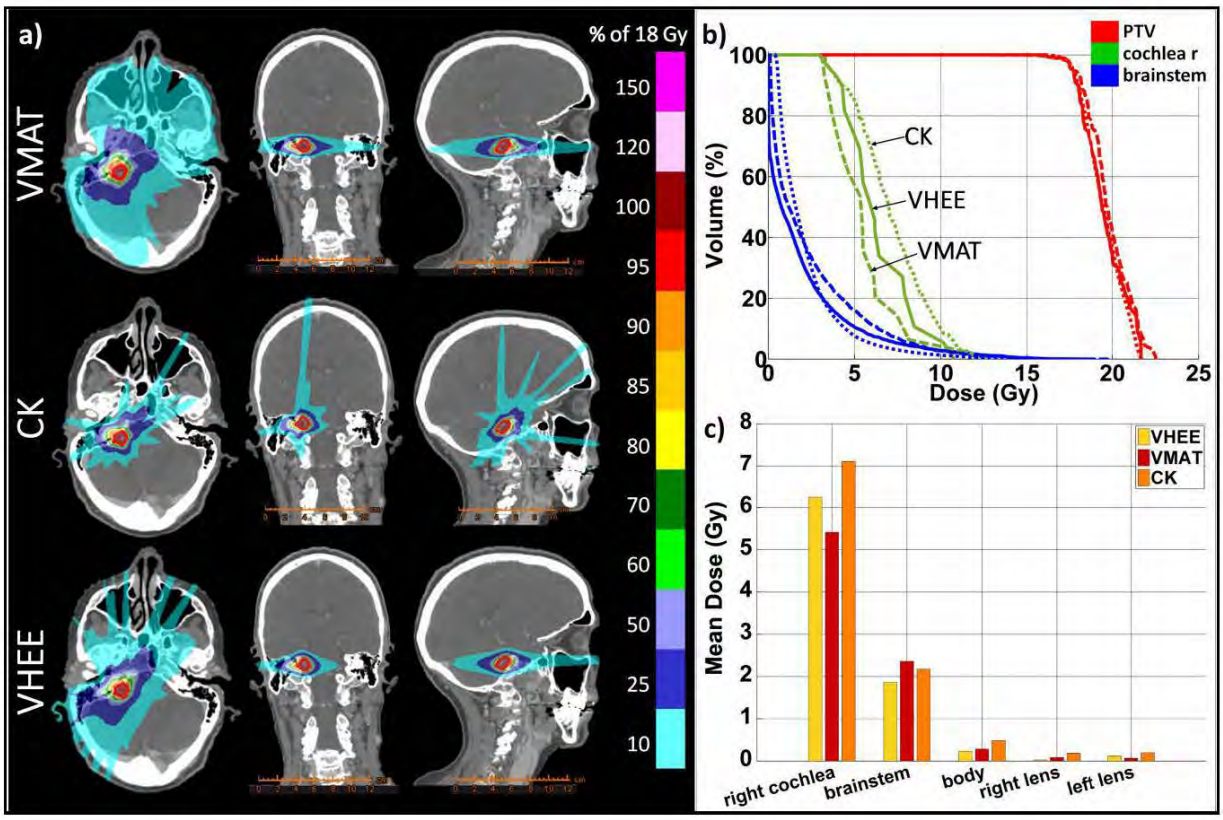
a)
VMAT
CK
VHEE
% of 18 Gy
150
120
100
95
90
85
80
70
60
50
25
10
b)
PTV
cochlea r
brainstem
CK
VHEE
VMAT
Volume (%)
Dose (Gy)
c)
VHEE
VMAT
CK
Mean Dose (Gy)
right cochlea
brainstem
body
right lens
left lens

Table

Table 1. PTV volumes, prescription doses, and conformity indices CI_{100} and CI_{50} corresponding to the VHEE, VMAT and CK plans, for each of the studied clinical cases.

Clinical case	PTV (cm^3)	PD (Gy)	CI_{100}			CI_{50}		
			VHEE	VMAT	CK	VHEE	VMAT	CK
Anal	937.7	40	1.00	0.99	-	4.94	6.69	-
	990.4	45						
Esophagus	801.5	40	1.05	1.09	-	3.18	4.78	-
	337.9	50						
Lung	98.8	54	0.95	0.97	-	2.98	3.42	-
Liver	9.3	54	0.98	0.99	-	3.52	4.36	-
Acoustic	1.2	18	1.22	1.36	1.06	8.91	9.23	5.59

* PD: Prescription dose

Figure1
Click here to do.....,..loaj highresolution image

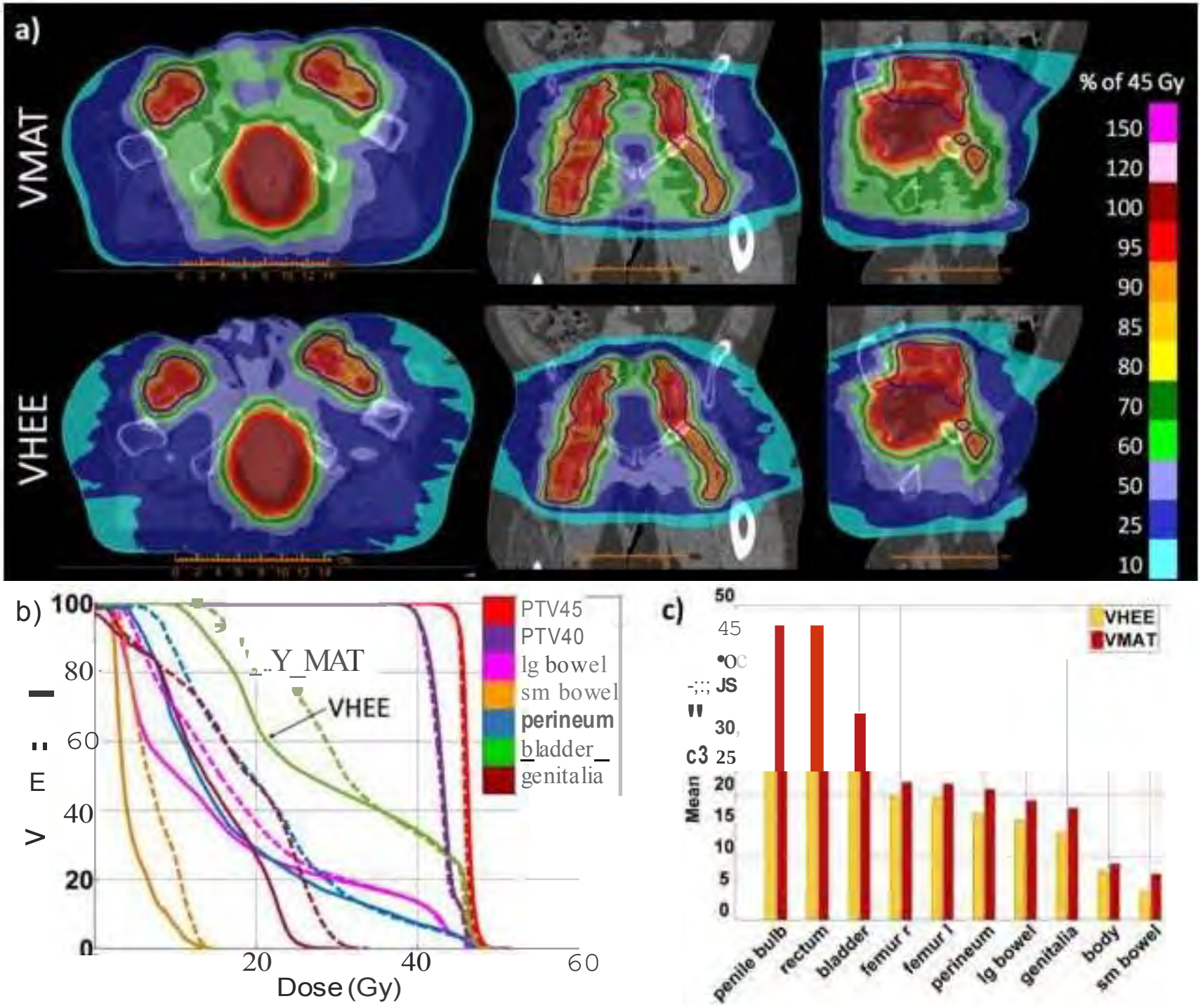

Figure2
Click here to do.....loaj high resolution image

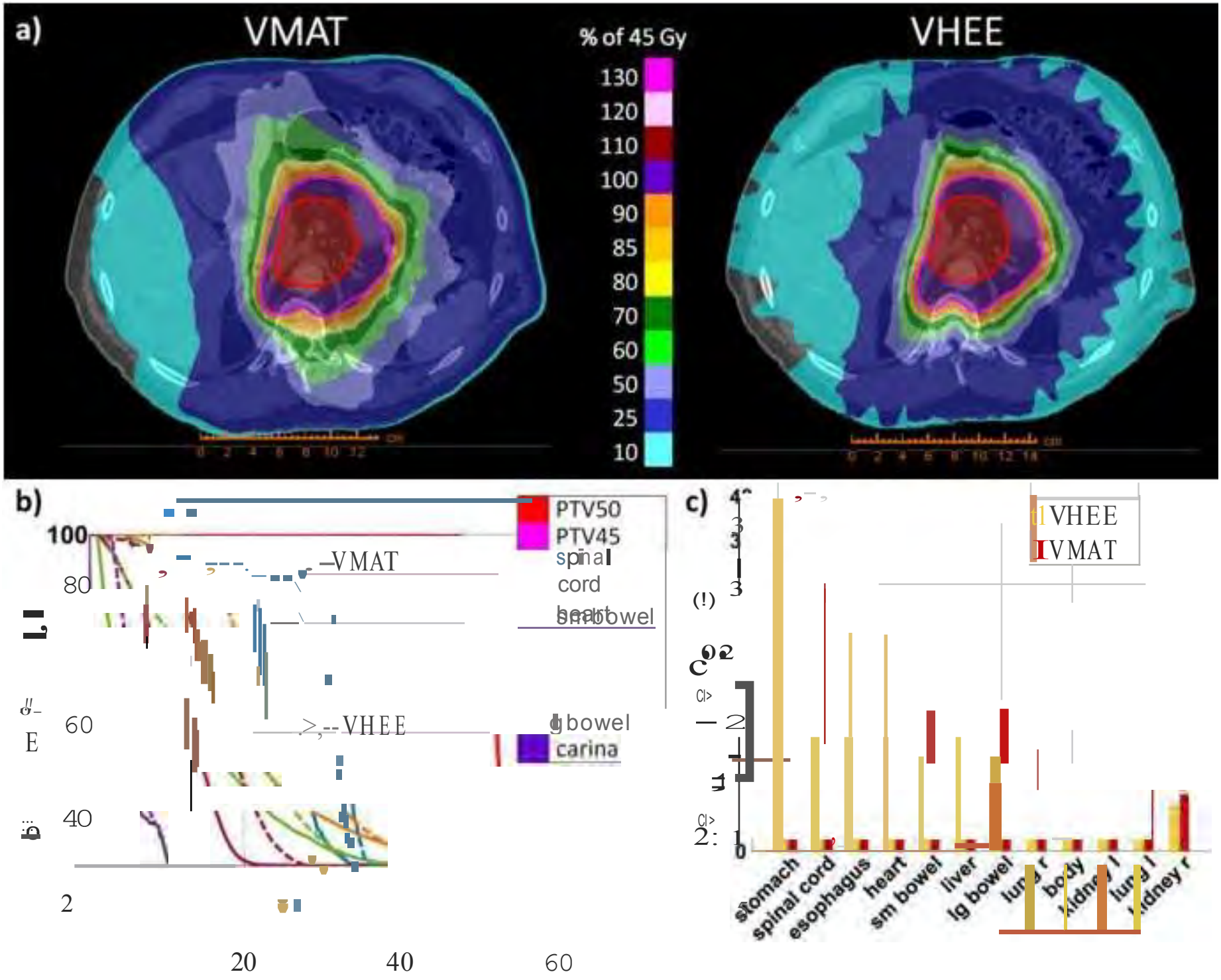

Dose (Gy)

Figure3
Click here to do.....,..loaj highresolution image

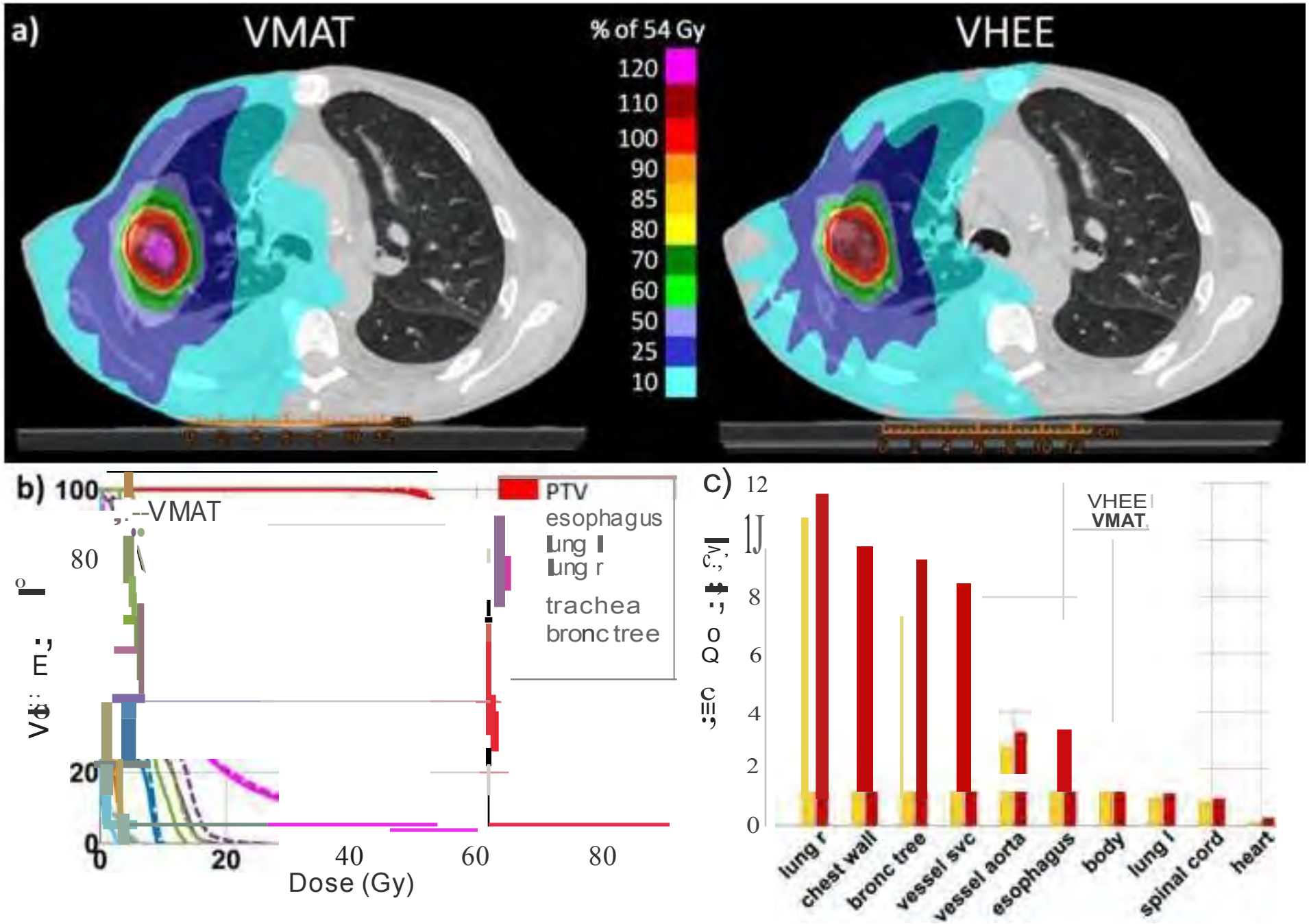

Figure4
Click here to do.....,..loaj highresolution image

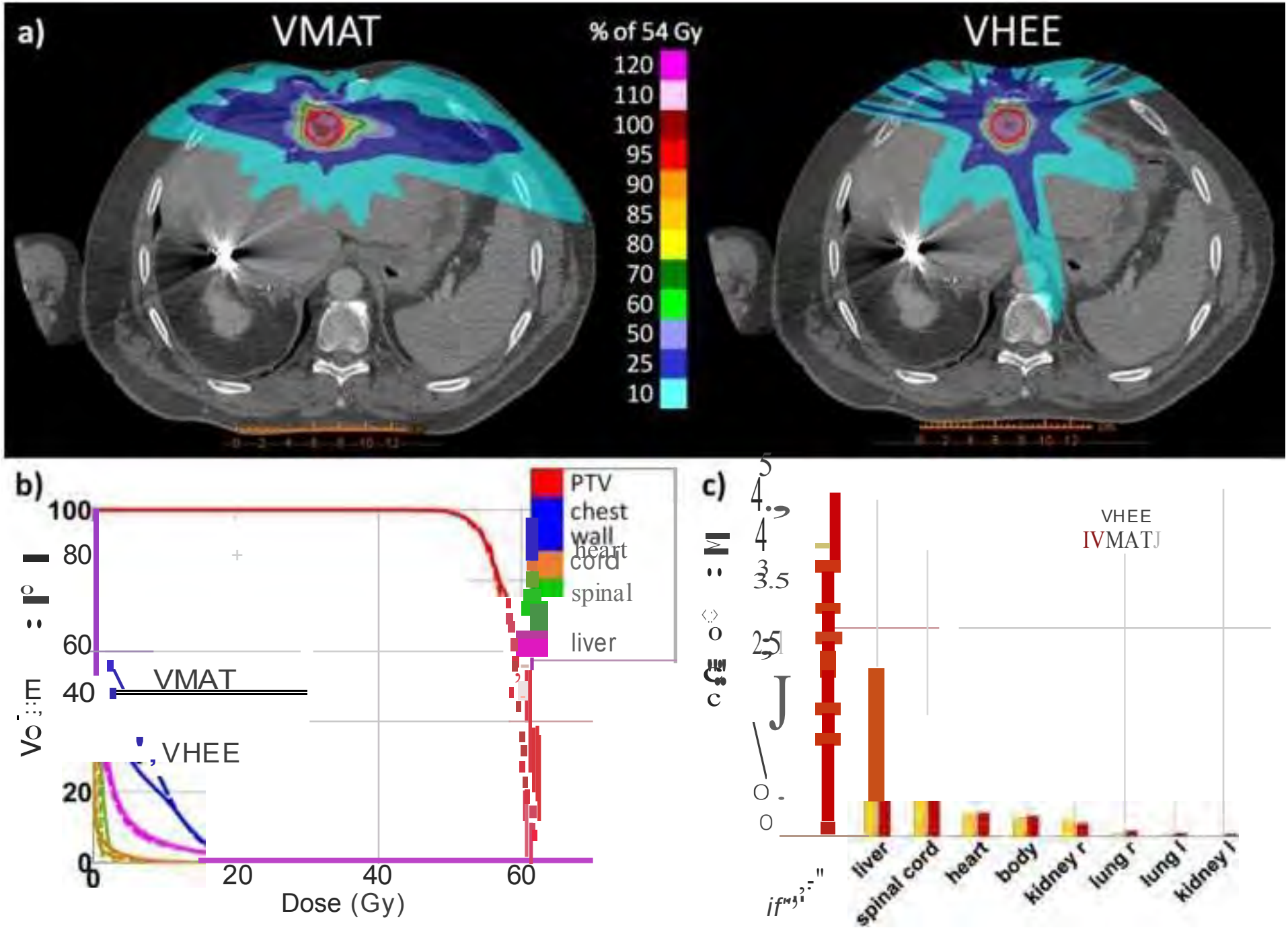

Figure 5
Click here to do.....loaj high resolution image

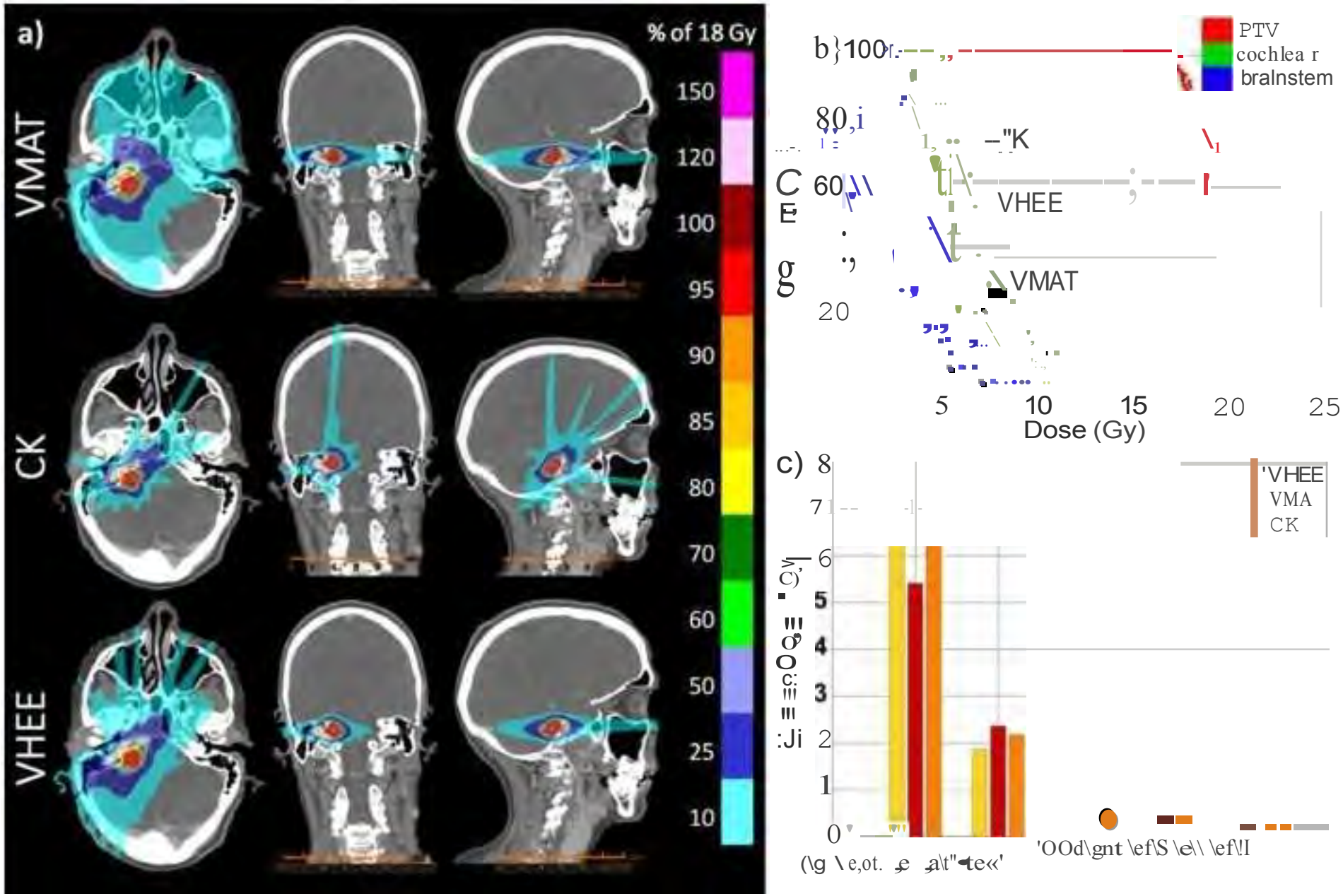

Conflict of Interest Statement

Bianey Palma, Bradley Qu and Magdalena Bazalova-Carter declare no conflicts of interest. Björn Hårdemark and Elin Hynning work for RaySearch Laboratories. Billy W. Loo and Peter G. Maxim have received research funding from Varian Medical Systems, speaking honoraria from Varian Medical Systems, and research support from RaySearch Laboratories. Billy W. Loo has also received research support from General Electric and Philips.

REPORT OF INVENTIONS AND SUBCONTRACTS

(Pursuant to "Patent Rights" Contract Clause) (See Instructions on back)

Form Approved
OMB No. 9000-0095
Expires Jan 31, 2008

PLEASE DO NOT RETURN YOUR COMPLETED FORM TO THE ABOVE ORGANIZATION. RETURN COMPLETED FORM TO THE CONTRACTING OFFICER.

1.a. NAME OF CONTRACTOR/SUBCONTRACTOR	c. CONTRACT NUMBER	2.a. NAME OF GOVERNMENT PRIME CONTRACTOR	c. CONTRACT NUMBER	3. TYPE OF REPORT *(X one)*
Peter Maxim, PhD	W81XWH-13-1-0165	Jamie Brazell	W81XWH-13-1-0165	a. INTERIM ☐ b. FINAL ☐

b. ADDRESS *(Include ZIP Code)*	d. AWARD DATE *(YYYYMMDD)*	b. ADDRESS *(Include ZIP Code)*	d. AWARD DATE *(YYYYMMDD)*	4. REPORTING PERIOD *(YYYYMMDD)*
THE LELAND STANFORD JUNIOR UNIVERSITY 450 Serra Mall Stanford, CA 94305-2004	20151115	820 Chandler Street Fort Detrick, MD 21702-5014	20151115	a. FROM 20131115 b. TO 20151114

SECTION I - SUBJECT INVENTIONS

5. "SUBJECT INVENTIONS" REQUIRED TO BE REPORTED BY CONTRACTOR/SUBCONTRACTOR *(If "None," so state)*

NAME(S) OF INVENTOR(S) *(Last, First, Middle Initial)* a.	TITLE OF INVENTION(S) b.	DISCLOSURE NUMBER, PATENT APPLICATION SERIAL NUMBER OR PATENT NUMBER c.	ELECTION TO FILE PATENT APPLICATIONS *(X)* d.				CONFIRMATORY INSTRUMENT OR ASSIGNMENT FORWARDED TO CONTRACTING OFFICER *(X)* e.	
			(1) UNITED STATES		(2) FOREIGN			
			(a) YES	(b) NO	(a) YES	(b) NO	(a) YES	(b) NO
None	None	None						

f. EMPLOYER OF INVENTOR(S) NOT EMPLOYED BY CONTRACTOR/SUBCONTRACTOR		g. ELECTED FOREIGN COUNTRIES IN WHICH A PATENT APPLICATION WILL BE FILED	
(1) (a) NAME OF INVENTOR *(Last, First, Middle Initial)* N/A	(2) (a) NAME OF INVENTOR *(Last, First, Middle Initial)*	(1) TITLE OF INVENTION	(2) FOREIGN COUNTRIES OF PATENT APPLICATION
(b) NAME OF EMPLOYER N/A	(b) NAME OF EMPLOYER		
(c) ADDRESS OF EMPLOYER *(Include ZIP Code)* N/A	(c) ADDRESS OF EMPLOYER *(Include ZIP Code)*		

SECTION II - SUBCONTRACTS *(Containing a "Patent Rights" clause)*

6. SUBCONTRACTS AWARDED BY CONTRACTOR/SUBCONTRACTOR *(If "None," so state)*

NAME OF SUBCONTRACTOR(S) a.	ADDRESS *(Include ZIP Code)* b.	SUBCONTRACT NUMBER(S) c.	FAR "PATENT RIGHTS" d.		DESCRIPTION OF WORK TO BE PERFORMED UNDER SUBCONTRACT(S) e.	SUBCONTRACT DATES *(YYYYMMDD)* f.	
			(1) CLAUSE NUMBER	(2) DATE *(YYYYMM)*		(1) AWARD	(2) ESTIMATED COMPLETION
N/A							

SECTION III - CERTIFICATION

7. CERTIFICATION OF REPORT BY CONTRACTOR/SUBCONTRACTOR *(Not required if: (X as appropriate))* ☐ **SMALL BUSINESS or** ☐ **NONPROFIT ORGANIZATION**

I certify that the reporting party has procedures for prompt identification and timely disclosure of "Subject Inventions," that such procedures have been followed and that all "Subject Inventions" have been reported.

a. NAME OF AUTHORIZED CONTRACTOR/SUBCONTRACTOR OFFICIAL *(Last, First, Middle Initial)*	b. TITLE	c. SIGNATURE	d. DATE SIGNED
Peter Maxim, PhD	Assistant Professor of Radiation Physics		20150701

DD FORM 882, JUL 2005 PREVIOUS EDITION IS OBSOLETE. Reset FormFlow/Adobe Professional 6.0

DD FORM 882 INSTRUCTIONS

GENERAL

This form is for use in submitting INTERIM and FINAL invention reports to the Contracting Officer and for use in reporting the award of subcontracts containing a "Patent Rights" clause. If the form does not afford sufficient space, multiple forms may be used or plain sheets of paper with proper identification of information by item number may be attached.

An INTERIM report is due at least every 12 months from the date of contract award and shall include (a) a listing of "Subject Inventions" during the reporting period, (b) a certification of compliance with required invention identification and disclosure procedures together with a certification of reporting of all "Subject Inventions," and (c) any required information not previously reported on subcontracts containing a "Patent Rights" clause.

A FINAL report is due within 6 months if contractor is a small business firm or domestic nonprofit organization and within 3 months for all others after completion of the contract work and shall include (a) a listing of all "Subject Inventions" required by the contract to be reported, and (b) any required information not previously reported on subcontracts awarded during the course of or under the contract and containing a "Patent Rights" clause.

While the form may be used for simultaneously reporting inventions and subcontracts, it may also be used for reporting, promptly after award, subcontracts containing a "Patent Rights" clause.

Dates shall be entered where indicated in certain items on this form and shall be entered in six or eight digit numbers in the order of year and month (YYYYMM) or year, month and day (YYYYMMDD). Example: April 2005 should be entered as 200504 and April 15, 2005 should be entered as 20050415.

1.a. Self-explanatory.

1.b. Self-explanatory.

1.c. If "same" as Item 2.c., so state.

1.d. Self-explanatory.

2.a. If "same" as Item 1.a., so state.

2.b. Self-explanatory.

2.c. Procurement Instrument Identification (PII) number of contract (DFARS 204.7003).

2.d. through 5.e. Self-explanatory.

5.f. The name and address of the employer of each inventor not employed by the contractor or subcontractor is needed because the Government's rights in a reported invention may not be determined solely by the terms of the "Patent Rights" clause in the contract.

Example 1: If an invention is made by a Government employee assigned to work with a contractor, the Government rights in such an invention will be determined under Executive Order 10096.

Example 2: If an invention is made under a contract by joint inventors and one of the inventors is a Government employee, the Government's rights in such an inventor's interest in the invention will also be determined under Executive Order 10096, except where the contractor is a small business or nonprofit organization, in which case the provisions of 35 U.S.C. 202(e) will apply.

5.g.(1) Self-explanatory.

5.g.(2) Self-explanatory with the exception that the contractor or subcontractor shall indicate, if known at the time of this report, whether applications will be filed under either the Patent Cooperation Treaty (PCT) or the European Patent Convention (EPC). If such is known, the letters PCT or EPC shall be entered after each listed country.

6.a. Self-explanatory.

6.b. Self-explanatory.

6.c. Self-explanatory.

6.d. Patent Rights Clauses are located in FAR 52.227.

6.e. Self-explanatory.

6.f. Self-explanatory.

7. Certification not required by small business firms and domestic nonprofit organizations.

7.a. through 7.d. Self-explanatory.